Title: Two common and distinct forms of variation in human functional brain networks

Authors: Ally Dworetsky[1,7], Benjamin A. Seitzman[2], Babatunde Adeyemo[3], Derek M. Smith[7], Steven E. Petersen[1,3,4,5,6], Caterina Gratton[7-9]

Affiliations:
Departments of Radiology[1], Radiation Oncology[2], Neurology[3], Psychological and Brain Sciences[4], Neuroscience[5], and Biomedical Engineering[6] – Washington University School of Medicine
Departments of Psychology[7], Neurology[8], Interdepartmental Neuroscience Program[9] – Northwestern University

Acknowledgements:
Funding was provided by NIH grant R01MH118370 (CG) and the James S. McDonnell Foundation (SEP).

Abstract

The cortex has a characteristic layout with specialized functional areas forming distributed large-scale networks. However, substantial work shows striking variation in this organization across people, which relates to differences in behavior. While a dominant assumption is that cortical 'variants' represent boundary shifts in the borders between regions, here we show that variants can also occur at a distance from their typical position, forming ectopic intrusions. Both forms of variants are common across individuals, but the forms differ in their location, network linkages, and activations during tasks. Sub-groups of individuals share similar variant properties, but sub-grouping on the two variant forms appears independent. This work argues that individual differences in brain organization commonly occur in two dissociable forms, border shifts and ectopic intrusions, that must be separately accounted for in the analysis of cortical systems across people. This work expands our knowledge of cortical variation in humans and helps reconceptualize the discussion of how cortical systems variability arises and links to individual differences in behavior.

1. INTRODUCTION

The cortex shows a characteristic organization, with distinct functional areas linking together to form distributed large-scale systems (or networks; (Churchland and Sejnowski, 1988)). This organization follows a stereotyped general pattern, but is not completely uniform, varying both across and within species. Comparative neuroanatomy studies demonstrate that variations in cortical organization appear in a constrained set of possible forms, including changes in the relative size, connectivity, or functional characteristics of cortical fields (Kaas, 2012; Krubitzer and Seelke, 2012). Notably, similar variation in cortical organization also exists within a species and can be influenced by genetic and developmental factors (Anderson et al., 2021; Krubitzer and Prescott, 2018). Variation in cortical organization relates to differences in phenotypic characteristics and behavior (Krubitzer and Seelke, 2012), suggesting that studying variation in cortical functional architecture in humans may provide insights into the link between neurobiology and behavioral traits relevant to cognition and disease.

The regional and systems-level organization of the human brain can be mapped non-invasively using functional connectivity MRI (*fcMRI;* correlations in the spontaneous activity patterns between different regions). FcMRI can be used to identify functionally homogenous regions (Eickhoff et al., 2018; Gordon et al., 2016; Wig et al., 2014) and distinct systems (Power et al., 2011; Yeo et al., 2011), that correspond well to patterns detected with task activation methods. For large groups of individuals, a "typical" average pattern of distributed functional systems emerges that is reproducible across studies and maps onto differences in motor, sensory, and higher-level processing (Power et al., 2011; Yeo et al., 2011).

However, recent work has also highlighted that any given person differs from this group pattern, at least in some locations (Finn et al., 2015; Gordon et al., 2017a; Gordon et al., 2017b; Gordon et al., 2017c; Kong et al., 2019; Laumann et al., 2015; Miranda-Dominguez et al., 2014; Mueller et al., 2013; Seitzman et al., 2019; Smith et al., 2015). We recently characterized locations, that we call *network variants*, where an individual's functional connectivity pattern differs markedly from the typical group average (with similarity below $r<0.3$) (Seitzman et al., 2019)[1]. Across multiple datasets, we demonstrate that network variants are stable over time (and across task states; (Kraus et al., 2021)) and relate to individual differences in brain activations during tasks and in behavioral measures collected outside of the scanner (Seitzman et al., 2019). Moreover, sub-groups of individuals show similarities in their network variants (i.e., with one group having network variants associated with top-down control and sensorimotor systems, and another sub-group showing network variants associated with the default mode system). We hypothesize that network variants reflect trait-like variations in the organization of functional brain areas across individuals (Seitzman et al., 2019).

[1] Network variant locations are present even after surface-based normalization procedures (Fischl, 2012; Klein et al., 2010; Van Essen, 2005) that align data across people by large-scale sulcal features; with individual differences in fcMRI not well related to variations in anatomical metrics ((Seitzman et al., 2019; Gordon et al., 2016) – although it is possible that they relate to finer-scale anatomical features, e.g., see (Miller et al., 2021)). This, together with correspondence to task responses, suggests that variants may relate more closely to differences in the functional positions of brain areas or systems, which can vary relative to anatomical landmarks (Frost & Goebel, 2012; Van Essen, Glasser, et al., 2012).

While a number of studies have identified locations of individual differences (Finn et al., 2015; Gordon et al., 2017a; Gordon et al., 2017b; Gordon et al., 2017c; Kong et al., 2019; Laumann et al., 2015; Miranda-Dominguez et al., 2014; Mueller et al., 2013; Seitzman et al., 2019; Smith et al., 2015), there has not been a substantial effort to characterize the different forms that these variants take and how they might link to sources and mechanisms observed in past comparative studies of cortical neuroanatomy in other species (Krubitzer and Seelke, 2012). Much work treats all forms of cortical variation uniformly, assuming that they are primarily driven by boundary shifts in the borders between systems: a functional region may expand, contract, or be slightly offset relative to the typical pattern (e.g., as has been documented for V1, which can differ more than 2-fold in size across individuals (Dougherty et al., 2003; Frost and Goebel, 2012)). Border shifts are likely important for understanding individual differences in behavior and brain function (Cui et al., 2020; Kong et al., 2019; Kong et al., 2021), and could potentially be addressed through functional alignment methods that allow for individually-specific regions to be locally displaced (e.g., (Haxby et al., 2011; Kong et al., 2021)).

However, it is possible that brain organization can also differ more markedly from the stereotypical pattern, with ectopic intrusions, islands of idiosyncratic fcMRI occurring in locations remote from their typical system organization (Gordon and Nelson, 2021). Evidence of dramatic shifts in the function or connectivity of primary sensory/motor areas can be seen with systematic deprivations in development (Arcaro et al., 2017; Krubitzer and Prescott, 2018; Striem-Amit et al., 2015), but it is less well understood how common these shifts are in higher-level association areas in neurotypical humans – despite some prior observations that they occur (Laumann et al., 2015; Seitzman et al., 2019). Ectopic intrusions are not easily explained by cortical expansion mechanisms and will be poorly addressed by functional alignment techniques that assume only local displacements in brain architecture, confounding group studies.

The goal of this study was to examine the relative prevalence of ectopic intrusions and border shift variants in humans, and to contrast the properties of these two forms of idiosyncratic variation. We used a combination of the Midnight Scan Club, a highly sampled "precision" fMRI dataset with 10 individuals scanned 10 times each, and the Human Connectome Project (HCP), a dataset of N= 384 with >45 min. of data. We demonstrate that both border shifts and ectopic intrusions are common characteristics of individual brain organization, but that these two forms of variation differ along a number of dimensions (spatial distribution, network association, functional activation, and sub-grouping of individuals). These findings add to our understanding of variation in human cortical organization and their constraints, providing evidence that variation comes in multiple dissociable forms. Separating these forms will likely be essential to deepening our understanding of the sources and consequences of individual differences in human brain organization and their relevance to clinical disorders.

2. RESULTS

Using a combination of the precision MSC dataset (N = 9, scanned 10 times each) and the large HCP dataset (N = 384), we investigated two different forms of idiosyncratic variations in functional system organization: variations associated with nearby shifts in the boundaries between a person's network organization and the typical layout ("border" shift variants) and

more remote islands of functional networks not adjacent to their typical layout ("ectopic" intrusion variants; see Supp. Fig. 1 and *Methods* for information on how both forms of variants are defined). We first examined how common ectopic intrusions were relative to border shifts variants across participants. We next asked how the two variant forms compare in their spatial occurrence, the networks they are affiliated with, and how they respond during tasks. Finally, we examined whether sub-groups of individuals showed similar forms of border and ectopic variants.

2.1. Nearly all individuals exhibit both border and ectopic cortical variants

Our first goal was to establish how frequently each of these network variant forms occur. Both ectopic variants and border variants were consistently identified in almost all individuals in both the MSC and the HCP datasets (at least one ectopic variant and at least one border variant were observed in all 9 of 9 MSC subjects and in 381 of 384 HCP subjects). In the HCP, an average of 42.6% [±14.8%] of an individual's network variants were ectopic; in the MSC, an individual's variants were 49.9% [±10.4%] ectopic on average (see Fig. 1A). As can be seen, the specific proportion of border and ectopic variants differed somewhat across individuals (Fig. 1, Supp. Fig. 2), but did not correlate with the total number of variants within an individual ($r = 0.04$ in the HCP dataset and $r = 0.15$ in the MSC). Interestingly, increasing the distance criteria (from 3.5 to 5, 7.5, or 10 mm) still left a large proportion of ectopic variants, with roughly 30% of variants classified as ectopic at 10 mm (Fig. 1B). Indeed, the median distance between ectopic variants and their own network was > 15 mm (Supp. Fig. 3). Thus, distant ectopic variants are not rare phenomena and, along with border variants, appear to be relatively ubiquitous at the individual level.

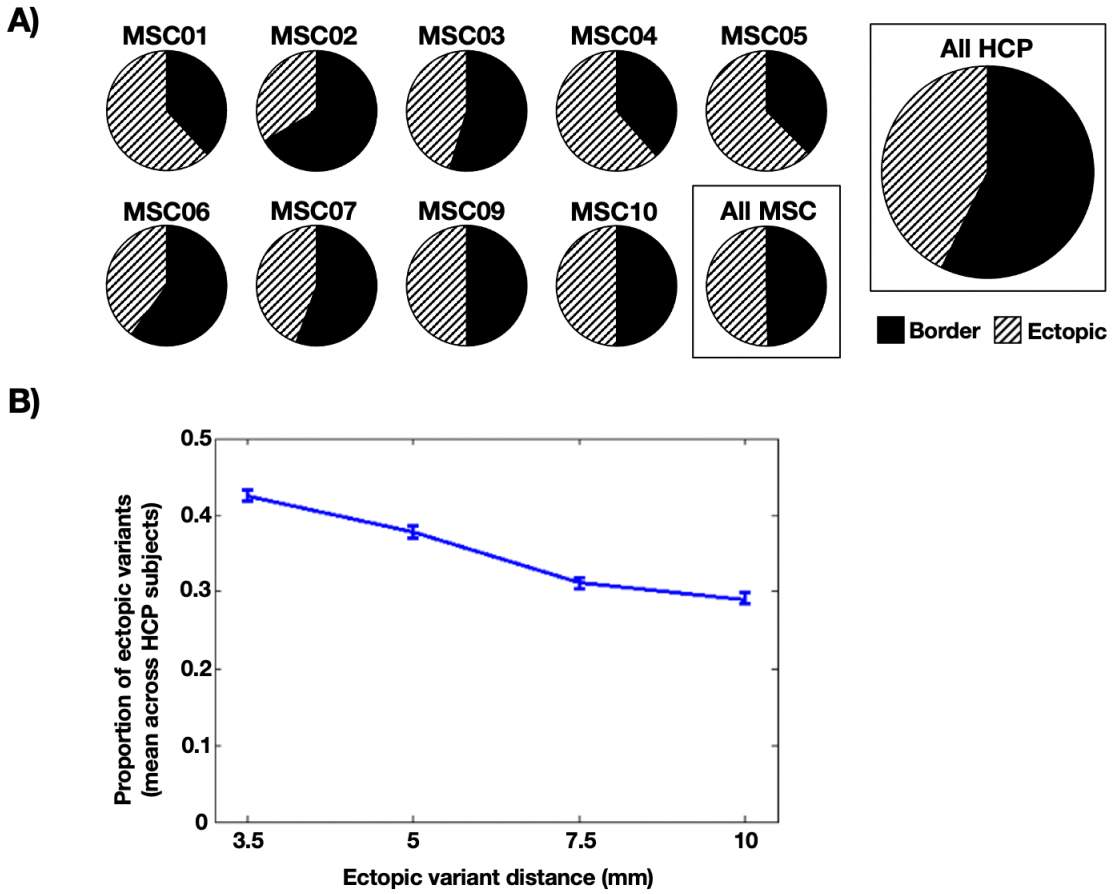

Fig. 1: Prevalence of border and ectopic variants across individuals. (A) The panel displays the proportion of border and ectopic variants within subjects in the MSC dataset (two rows on left), and across all subjects in the HCP dataset (far right). Both ectopic variants and border variants were consistently identified in almost all individuals in both the MSC and the HCP datasets. (B) Proportions of ectopic variants at other distances. As the required minimum distance for a variant to be classified as ectopic increases to 5, 7.5, and 10 mm, ectopic variants continue to comprise a sizable percentage of all variants in the HCP dataset, nearly 30% even at a distance of 10 mm. Error bars represent SEM across participants. (See Supp. Fig. 4 for spatial distributions of border and ectopic variants at each of these distance thresholds.)

2.2. Border and ectopic variants are spatially distinct

Next, we asked whether ectopic and border variants tend to occur in different locations. We examined the spatial overlap of ectopic variants and compared it to the overlap of border variants. The spatial distributions of the two variant forms are shown in Figure 2A, where warmer colors represent brain regions with a high occurrence of variants across subjects. While both forms of variants follow the general distribution previously described (Seitzman et al., 2019) of higher prevalence in association regions of cortex (especially in lateral frontal cortex, superior frontal cortex and near the temporoparietal junction), it appears that ectopic variants have a distinct distribution relative to border shifts.

To test for the significance of these differences, we conducted a permutation test where ectopic and border labels were randomly shuffled for each variant within subjects and used to create 1000 permuted overlap maps. The true maps were then compared to these permuted maps. The true ectopic and border variant maps were significantly more dissimilar than the permuted maps ($p < 0.001$; none of the permuted maps were as dissimilar as the true overlap maps, Figure 2B). A similar permutation approach was used to create a multiple comparisons cluster-corrected Z-map ($p < 0.05$, see *Methods*), revealing several key locations that differed in the frequency with which the two variant forms appeared. As shown in Figure 2C, ectopic variants appear more frequently in dorsolateral frontal regions of the right hemisphere, whereas border variants are more frequent around rostral portions of temporoparietal junction and superior rostral frontal regions in both hemispheres (see Supp. Fig. 4 for similar results with ectopic variants defined at longer distances).

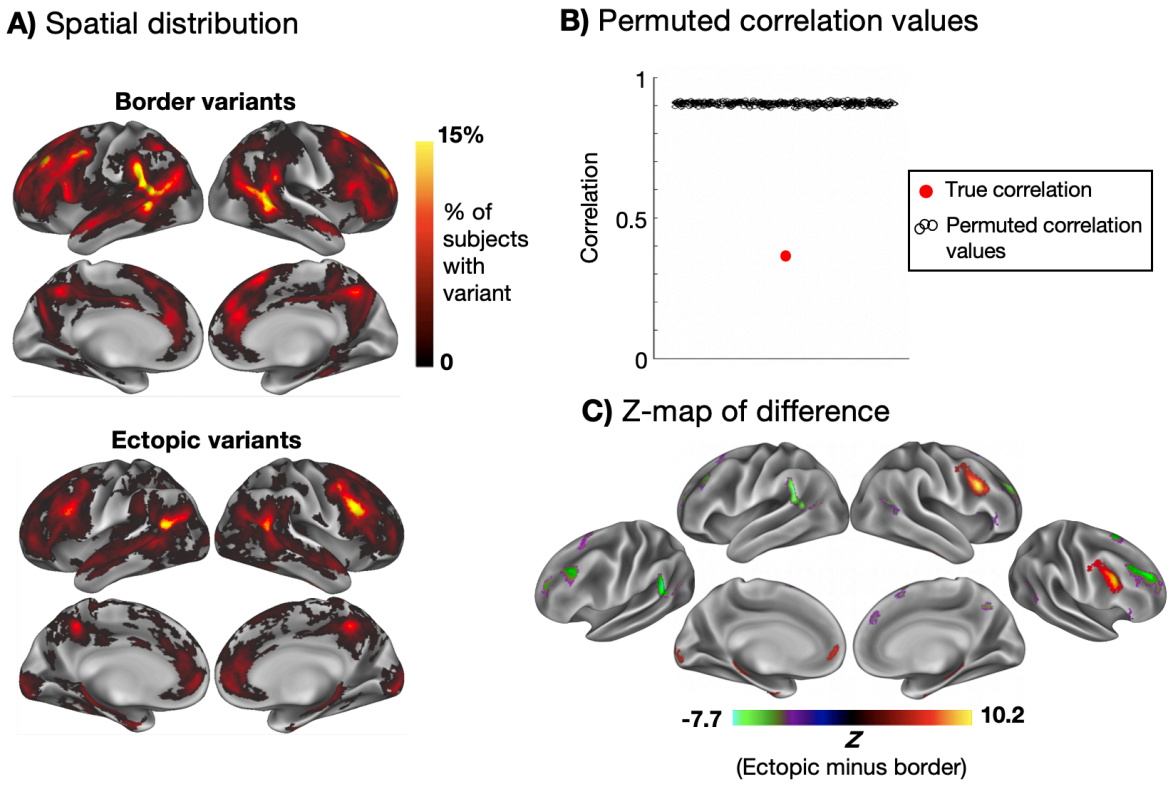

Fig. 2: Spatial distributions of ectopic and border variants. The maps in (A) show the spatial distribution of border variants and ectopic variants, overlapped across participants in the HCP. (B) These two spatial distributions differ significantly more than expected by chance from random permutations. (C) A Z-map is shown highlighting regions with a significantly higher occurrence of border variants (green/purple) and ectopic variants (yellow/red; $p < 0.05$ cluster-corrected for multiple comparisons based on permutation testing). Ectopic variants were more prevalent in the right posterior inferior frontal sulcus and left posterior TPJ regions, while border variants were more prevalent in dorsal and ventral portions of the anterior TPJ and superior rostral frontal regions. See Supp. Fig. 4 for evidence of similar results for ectopic variants at greater distances.

2.3. Border and ectopic variants exhibit different patterns of network assignment

We next examined the network assignments of each variant form (see Supp. Fig. 5 for network templates used in this analysis; as described in the *Methods*, variants were "assigned" to a network based on which template best fit that variant's seedmap). As a general pattern, variants tend to frequently be associated with the default mode, fronto-parietal, and cingulo-opercular networks across both datasets, consistent with previously reported results (Figure 3A, Supp. Fig. 6; note that in the MSC, many variants are also associated with the Language network, but this network template was not identified in the HCP dataset; see *Methods*). In both datasets, when separated based on form, we found that ectopic variants have a distinct frequency of network assignment relative to border variants.

In the HCP dataset, border variants appeared more commonly linked to the default mode network (DMN), fronto-parietal (FP), and parieto-occipital network (PON). Ectopic variants were relatively more linked to the dorsal attention (DAN), parietal memory (PMN), and sensorimotor networks (visual, somatomotor, auditory). Permutation testing of variant labels in the HCP dataset confirmed these observations (Fig. 3B). As may be expected, ectopic variants were relatively more abundant in smaller or more spatially local networks, as it is easier to be distant from these network boundaries. However, ectopic variants were still often associated with large networks such as the DMN, FP, cingulo-opercular (CO), DAN, and Visual systems, emphasizing their common nature. Distributions of variant network assignments in the MSC are shown in Supp. Fig. 6; the smaller number of variants in the MSC led to greater variability in per-network proportions of variant forms, but still consistently found evidence of ectopic variants associated with many large (and small) networks.

Interestingly, combining information from the spatial and network analysis, one can find that border and ectopic variants often exhibited systematic "swaps" in their territory relative to the canonical structure (see Supp. Fig. 7). For example, border variants located in canonical fronto-parietal territory most often are re-assigned to DMN, CO, or DAN. Thus, while idiosyncratic, both forms of variants show constraints in how they vary.

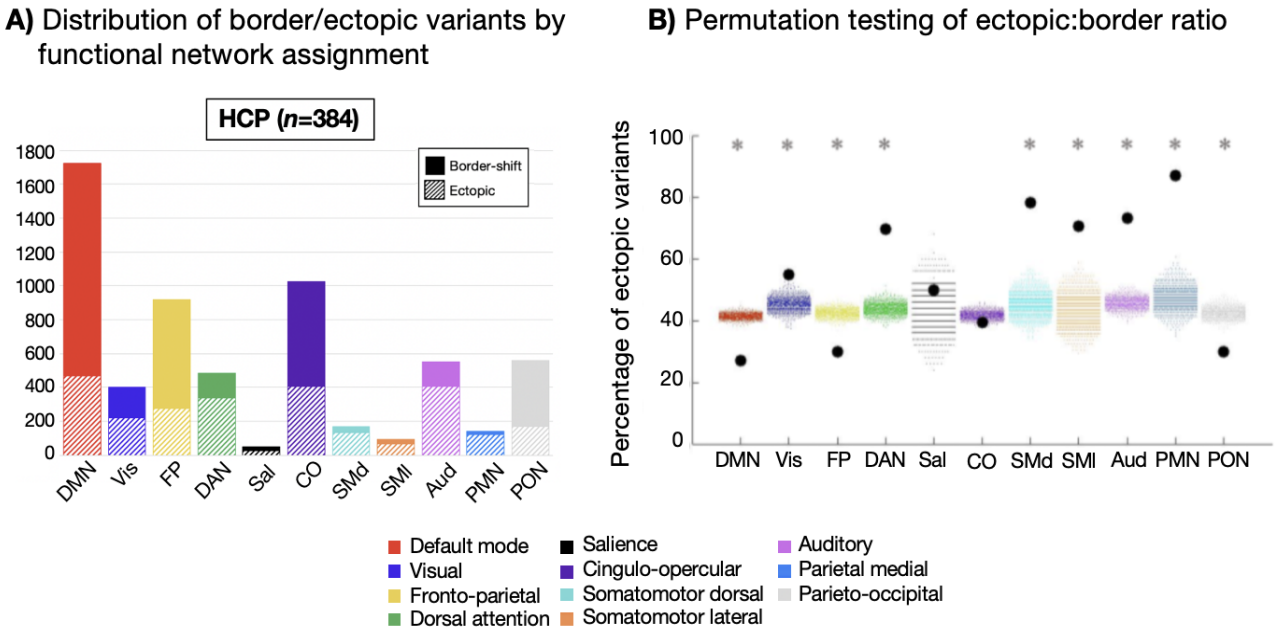

Fig. 3: Network linkages of border and ectopic variants (A) Network distributions of border and ectopic variants in the HCP dataset. Variants of both forms are commonly associated with the DMN, FP, and CO networks, as reported in past work (Seitzman et al., 2019). (B) Plot depicting permutation testing of the ectopic:border ratio in the HCP dataset. For all networks with the exception of salience and cingulo-opercular, the true proportion of ectopic variants (black dots) was significantly different from permuted proportions (colored dots, 1000 random permutations of shuffled labels) at $p<0.001$ (*; FDR corrected for multiple comparisons). DMN, FP, and PON variants were more likely to be border shifts, while sensorimotor, DAN, and PMN variants were more likely to be ectopic. Notably, ectopic variants were commonly found in all systems. See Supp. Fig. 5 for cortical depiction of each listed network.

2.4. Border and ectopic variants exhibit shifted functional profiles

Next, we asked if both forms of variants show altered task responses, consistent with their idiosyncratic network profile. We begin by testing common task positive and negative responses. Following Seitzman et al. (2019) (where activations were tested for all activations as a whole), we focused on the mixed design task from the MSC. This design consisted of blocks of noun/verb judgments on presented words and blocks of dot coherence concentricity judgments. Average activations (in all cues/trials and blocks) were contrasted with baseline (see *Methods* for details), a contrast that elicits negative activations in DMN regions typically, and positive activations in the FP, DAN, and visual systems.

Both ectopic variants and border variants exhibit shifted functional profiles, in the direction expected for canonical regions associated with the same network (Figure 4A). Border variants are shifted further toward the expected activation based on their new assignment than ectopic variants: while we observe a strong task deactivation for border DMN variants ($t(7) = -5.38$, $p = 0.001$ for 8 MSC participants with border DMN variants), aligning closely with canonical DMN deactivation, ectopic DMN variants exhibit a relatively weaker (but still significant) deactivation ($t(6) = -2.76$, $p = 0.033$ for 7 MSC participants with ectopic DMN variants). Similar patterns are seen with "task positive" networks like the visual, fronto-parietal, and dorsal attention networks; the cingulo-opercular, language, and salience networks were not strongly modulated by this contrast.

This finding is further examined in Figure 4B for each MSC participant by comparing the task activation of DMN variants in a given subject to that same variant location in other subjects. This analysis showed that – in every individual participant – similar patterns of prominent decreases in activations were observed relative to what is expected in that location in both ectopic variants ($t(6) = 5.99$, $p<0.001$) and border variants ($t(7) = 5.97$, $p<0.001$). However, the ectopic DMN variants appear in locations that have a more positive typical response pattern in comparison to border variants, and thus do not reach as strong a level of deactivation.

Jointly, these findings demonstrate that both ectopic and border variants are associated with shifted task activations, shifting toward the expected activations for the variants profile. Border variants associated with the default network retain a task activation profile similar to canonical locations, while ectopic variants show an altered but intermediate profile.

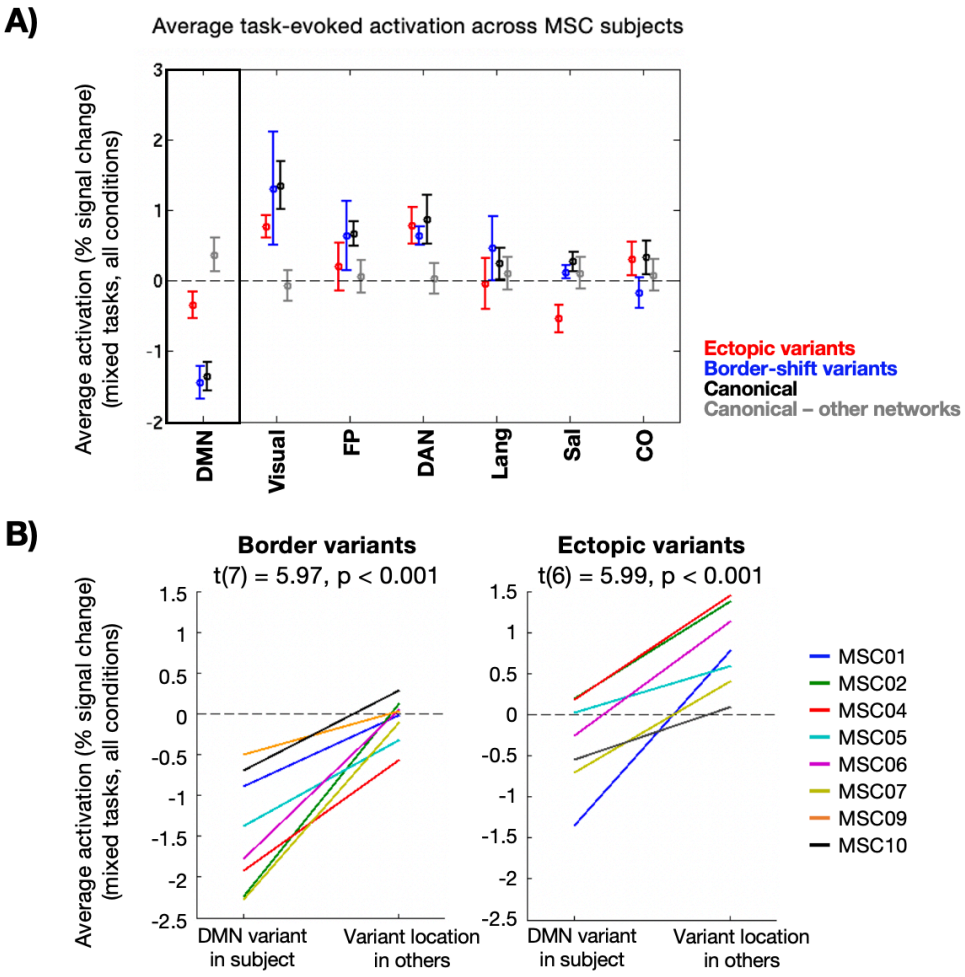

Fig. 4: Average task-evoked activation by network across MSC subjects. (A) Average activation (*z*) across all task conditions in a set of mixed-design tasks from the MSC for variants (red = ectopic, blue = border shift), canonical locations in the listed network (black), or canonical locations in other networks (gray). Error bars represent the standard error of the mean. (B) Average activation of DMN-assigned variants in an individual vs. average activation in that location in all other individuals for border (left) and ectopic (right) variants; 8 of 9 subjects with a border DMN variant and 7 of 9 subjects with an ectopic DMN variant were included. Different colors represent different MSC participants.

2.5. Both border and ectopic variants separate individuals into distinct subgroups

In (Seitzman et al., 2019), we found that network variants could be used to subgroup individuals, with two main reproducible clusters of individuals: those with variants more associated with the DMN and those with variants more associated with control and sensorimotor processing systems. Thus, our next question was whether similar subgroups would be evident for ectopic and border variants when examined separately. This analysis provides insight into the relative linkage or independence between the two variant forms

To this end, individuals in the HCP dataset were grouped based on variants' similarity to each of 11 network templates and then clustered into subgroups as in (Seitzman et al., 2019). This analysis was conducted on two matched split-halves of the HCP dataset to confirm the reproducibility of data-driven clustering findings. When the Infomap algorithm was applied to cluster individuals whose variants had similar network profiles (see *Methods*), we identified three consistent sub-groups of individuals in both border and ectopic variants (Fig. 5A and 5B, respectively).

In clustering individuals via their border variants, we found one large sub-group of individuals whose variants were more highly correlated with the DMN and less highly with control and processing networks (we refer to this sub-group as B1; 57% of subjects, green in Fig. 5A). The second large sub-group had border variants with an intermediate profile, associated with control systems (CO-, DAN-, and FP-like), with a low correlation to sensorimotor networks and the DMN (B2; 27% of subjects, black in Fig. 5A; note this subgroup is distinct from ones observed in our previous analyses). A third smaller sub-group included participants with more CO-like variants, with stronger associations to sensorimotor networks and low correlation to the DMN (B3; 15% of subjects, purple in Fig. 5C; this profile was similar to our second sub-group in previous work (Seitzman et al., 2019)).

Clustering individuals via ectopic variants resulted in three subgroups as well, but these differed in their specific characteristics. The first sub-group included people with ectopic variants that associated more strongly with FP and DMN and lower correlation to control networks (E1; 28% of subjects, light green in Fig. 5B; while similar to B1, note the less prominent DMN profile). A small intermediary sub-group had ectopic variants strongly associated with DMN, auditory and somatomotor networks, and less strongly with control networks (E2; 12% of subjects, gray in Fig. 5B; distinct from any of the border subgroups). The final and largest sub-group had strong associations to the CO, DAN, and PON networks (E3; 60% of subjects, pink in Fig. 5B; most similar to sub-group B3),

Notably, we found that individuals who were members of a particular sub-group in one variant form were not consistently sorted into the same sub-group according to the other variant form; i.e., a subject whose border variants assign them to the DMN-like B1 sub-group may not necessarily be assigned to the DMN-like E1 sub-group based on ectopic variants. To confirm this discrepancy, an additional analysis was performed in which each subject was forced into either DMN or control/processing clusters (as these were the most consistently identified across analyses) using a template approach (see *Methods* for more details). All HCP subjects with at least one border and one ectopic variant were included in this analysis (N=381/384). Cluster grouping was then compared for consistency. Figure 5C shows the results of this template-based sub-grouping. While an individual's sub-group based on border variants was relatively likely to be consistent with its overall (all variants) sub-group (adjusted Rand index = 0.31), sub-groups based on ectopic variants were independent of the sub-groups based on border (adjusted Rand index = -0.01) or all variants (adjusted Rand index = 0.09). This suggests that border and ectopic variant forms are relatively independent, appearing in distinct patterns across individuals.

As in the (Seitzman et al., 2019) paper, we tested for association with 6 behavioral HCP factors but did not find any significant differences (Supp. Fig. 8), suggesting that either these sub-groups

are not linked to these factors or that the effect sizes are too small to observe within the subset of HCP data analyzed here (Marek et al., 2019).

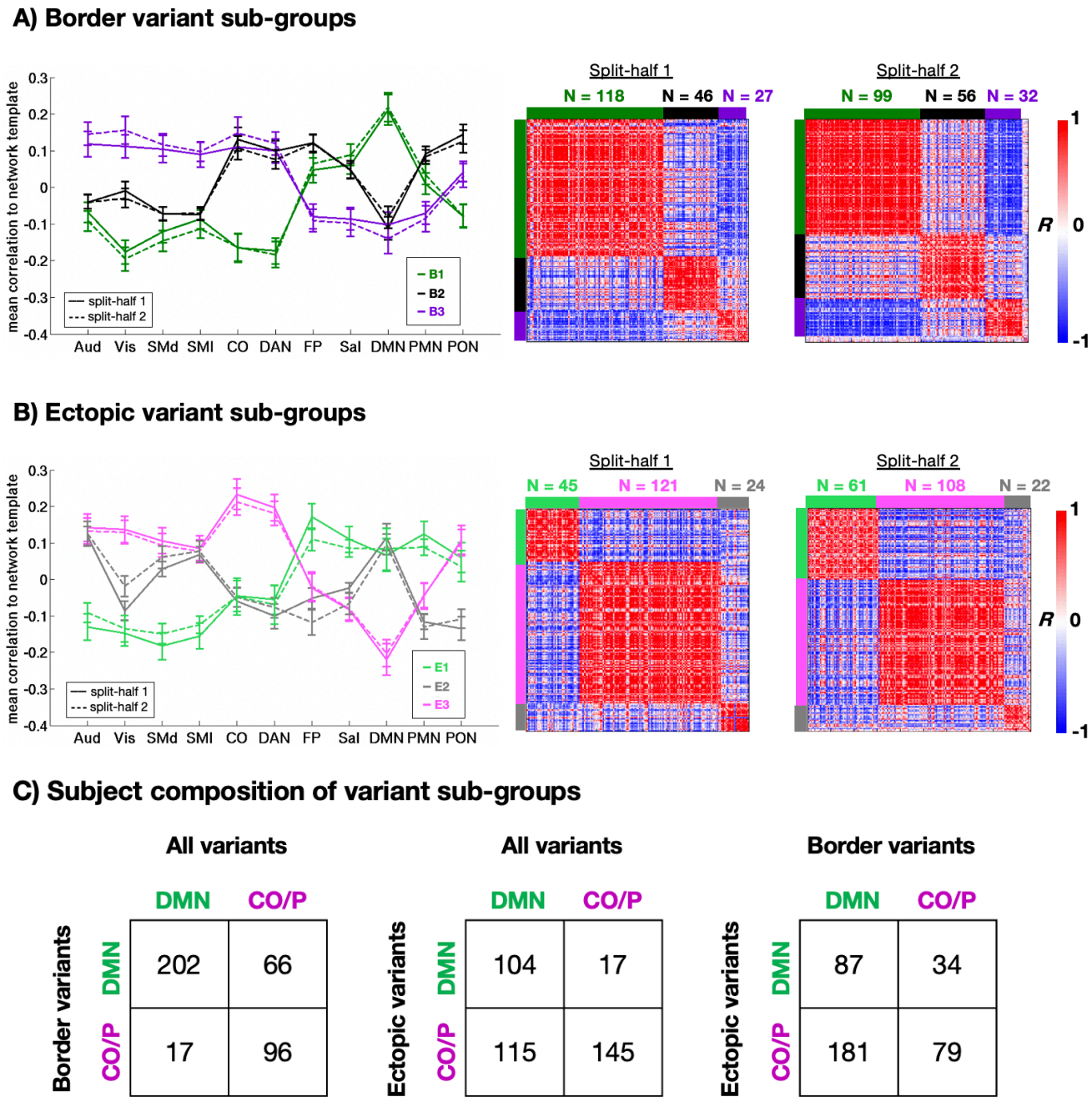

Fig. 5: Similarity of border and ectopic variants across sub-groups of individuals. For border variants (A) and ectopic variants (B), we separated individuals into sub-groups based on the average network profile of their variants (left). Matrices on the right show across-subject similarity (correlation) of variant profiles for each split-half in the HCP. Color blocks at the edges of the matrices denote the sub-group identities. The two variant forms produced three sub-groups each with high similarity across matched split-halves of

the HCP data. However, the sub-groups differed between the two forms. (C) Contingency tables show the composition of sub-groups in which each individual's variant profile (all variants, border variants only, and ectopic variants only) was forced to sort into either a DMN-like sub-group or a control/processing sub-group. Note that ectopic and border variant sub-group labels had poor association with one another.

3. DISCUSSION

While much previous work treats individual differences in brain networks as uniform, we observed that locations with idiosyncratic brain network "variants" come in two forms: shifts in the borders between adjacent systems and ectopic intrusions, islands of an atypical system at a distance from its usual location. Here, we used a combination of the precision MSC (N=9, 10 sessions each) and large HCP (N=384, 2 sessions each) datasets to investigate the prevalence and properties of each of these variant forms. We found that instances of both border and ectopic variants were found in almost all individuals in this dataset. While they shared some common features, they differed significantly on a number of properties when contrasted directly, including their spatial location, the networks they were associated with, and their functional responses during tasks. Across people, we found distinct sub-groups with shared variant properties that replicated across split-half samples of the dataset. Notably, however, sub-groups appeared independent across the two variant forms. Jointly, these findings suggest that variation in functional brain systems come in (at least) two dissociable forms that likely link to distinct underlying processes. Separation of these two forms is likely to provide new insights into the sources of individual differences and their implications for normative and clinical behavior.

3.1. Ectopic islands of variation are common properties of brain organization

A wealth of recent studies has provided evidence of individual differences in brain organization and linked these differences to cognitive variation (e.g., (Bijsterbosch et al., 2018; Cui et al., 2020; Kong et al., 2019)).These locations of individual differences are all typically treated equivalently, often with the assumption that they reflect differences in the topographic boundaries, or borders, between systems. However, our work suggests that variant brain locations come in different forms, not only associated with border shifts, but also with ectopic intrusions. Ectopic variants are in fact relatively common, present in all 9 MSC subjects and 381 of 384 HCP subjects and comprising ~40-50% of variants across both datasets. Even at further distances (e.g., 10mm from a similar network boundary) ~30% of variants were ectopic (see Fig. 1B; note that the median distance between ectopic variants and their canonical territory is > 15 mm, see Supp. Fig. 3). Thus, ectopic variants are not only common, but also many ectopic variants observed are fairly remote from their expected network boundaries. Many descriptions of individual differences in human brain systems discuss them with respect to boundary-related mechanisms (e.g., a region expanding or taking over territory in nearby locations) and distance-based functional alignments have been suggested as a. means to address these differences. However, different theories and approaches will be needed to address ectopic variation (see next sections).

Prior to this paper, the existence of ectopic variants had been hinted at in previous work. For instance, (Seitzman et al., 2019) and (Laumann et al., 2015) observed regions where an individual's functional network organization differs from a group-average description, including

regions where a network appeared more distant from its typically observed boundaries (e.g., see DMN variants in Fig. 4B of (Seitzman et al., 2019) and island of CO appearing in the individual-level map in Fig. 7 of (Laumann et al., 2015)). Similarly, work by (Glasser et al., 2016) parcellating the human cortex noted several instances of sizable spatial displacements in individual-level topography relative to a group-average representation. In this work, we build on these initial observations to systematically characterize the prevalence of ectopic variants and determine how they differ from border shifts along a number of dimensions.

Although common, the proportion of ectopic to border variants varied on a subject-to-subject basis; in the MSC dataset, for instance, some subjects had relatively fewer ectopic variants (i.e., ectopic variants in MSC02 and MSC06 comprised 33% and 40% of total network variants, respectively), whereas in some other subjects (e.g., MSC01, MSC04, and MSC05) the proportion of ectopic variants exceeded 60% (see Supp. Fig. 2 for a breakdown of these proportions in both datasets). Thus, ectopic variants, and more specifically the ratio of ectopic to border variants, may differ systematically across individuals.

3.2. Border shifts and ectopic intrusions are distinct forms of individual variation in brain organization

Comparative neuroanatomy studies have shown that cortical functional architecture can differ in a variety of ways across mammals, including differences in the cortical area size/position, number, organization, and connectivity (Krubitzer and Prescott, 2018). Although not as often discussed, many of these differences are also seen across individuals within a species (Krubitzer and Seelke, 2012). Linking to this work, we hypothesized (Gratton et al., 2020; Seitzman et al., 2019) that network variants represent a combination of border shifts (expansions, contractions, or displacements relative to the canonical cortical area layout, which will result in differences adjacent to their typical locations) and ectopic intrusions (islands of altered connectivity and function of a region[2] at a distance from the canonical organizational structure). Past work has suggested that even in the typical population, there is substantial variation in the size and position of specific human cortical areas (e.g., in V1 size (Dougherty et al., 2003) with potential links to functional differences in vision (Schwarzkopf et al., 2011; Verghese et al., 2014); in the position of Broca's area (Fedorenko and Blank, 2020; Juch et al., 2005)). Here we demonstrate that variations both close to and distant from the canonical system structure occur commonly across people and many brain regions, but that these two forms of variation differ along a number of dimensions (in spatial location, network assignment, task activations, and sub-

[2] Note that while we have made efforts to identify homogeneous network variant units, each network variant is not necessarily equivalent to a cortical area. Brain areas can be defined based on a combination of properties, including their function, architectonics, connectivity, and topography (FACT; (Van Essen & Glasser, 2018)). Network variants define idiosyncratic locations on the basis of functional connectivity alone (although with evidence that these regions also align with differences in task function, see Fig. 4); thus, in this sense these regions may be considered to align with distinct areas. However, consider the example of border shift variants: these variants could arise because an area within an individual has been expanded or displaced across a border to subsume territory of another region. Using our methods, only the non-overlapping segment will be labeled a variant. Therefore, even if functional connectivity were a perfect proxy for brain area divisions, these variants might represent only a subunit within the area.

grouping). These differences suggest that border and ectopic variants may link to differing underlying sources.

A number of different developmental factors influence how cortical functional systems are organized. Gradients in the expression of transcription factors in patterning centers of the cortex control the size and position of many cortical areas (O'Leary et al., 2007). It has been proposed that intrinsic genetic factors create "proto-areas" whose boundaries are refined and sharpened through experience-dependent mechanisms (Cadwell et al., 2019). Similar principles have been theorized to underlie the development of distributed cortical systems, starting from a proto-organization that is refined, fractionated, and sharpened with experience (DiNicola and Buckner, 2021).

Indeed, while some basic properties are preserved, profound differences in experiences (e.g., sensory deprivation during critical periods) have been shown to substantially alter cortical area size, layout, and connectivity in rodents (Krubitzer and Prescott, 2018). Similarly, experience with faces has been demonstrated to be critical to the formation of face selective areas in macaques, although basic retinotopic organization remains (Arcaro et al., 2017). In humans, functional connectivity of congenitally blind individuals shows intact internal topography but large differences in the interareal connectivity of these regions (Striem-Amit et al., 2015), while those born with only one hand show cortical expansions of regions representing motor functions of other body parts (Hahamy et al., 2017).

These studies in humans and non-human animal models help to explain how cortical organization can both demonstrate substantial commonalities across individuals, but also punctate locations of differences within a species - some associated with local changes (e.g., due to changes in area sizes, which would likely result in border variants), and others that could be linked to more distant alterations (e.g., strong changes in connectivity/function of a (sub)-region that may underlie ectopic variants). Network variants provide a robust and high-throughput approach to identify variants across the human brain, helping to constrain theories of the sources and consequences of cortical area variation.

3.3. Impact for basic research studies

At present, many resting-state and task-based fMRI studies aggregate or compare data across individuals based on spatial normalization, thus assuming that the same spatial layout of brain systems is conserved across individuals (Fedorenko, 2021). However, widespread individual differences in the localization of brain regions and systems may lead to detrimental effects when performing group-level analyses, including loss of sensitivity and functional resolution (Nieto-Castanon and Fedorenko, 2012), and prediction accuracy of task functional connectivity (Porter et al., 2021), task-evoked signals (Guntupalli et al., 2018; Haxby et al., 2020), and prediction of behavior from resting networks (Brennan et al., 2019; Fan et al., 2020; Kong et al., 2019; Kong et al., 2021). Together, these limitations lead group studies to fall short of providing comprehensive explanations of brain function and cognition as a whole.

Functional alignment across individuals may be improved by more accurate anatomical registration, such as via surface-based mapping methods (Fischl, 2012; Klein et al., 2010).

However, the resulting functional overlap may be variable depending on the level of cognitive function and brain area in question (Frost and Goebel, 2012; Van Essen et al., 2012a), with a bias toward enhancing the functional concordance of regions supporting lower-level cognitive processes (Tahmasebi et al., 2012). As an alternative, several approaches to increase cross-subject correspondence have been suggested based on improved alignment of functional signals themselves. This includes individualized approaches such as collecting functional localizer task data from each individual subject (Fedorenko, 2021; Fedorenko et al., 2013; Kanwisher et al., 1997; Saxe et al., 2006), adopting fcMRI methods to define brain systems and areas from subjects with large quantities of data (Braga and Buckner, 2017; Gordon et al., 2017c), or hyperalignment-based techniques to increase functional correspondence (Guntupalli et al., 2018; Haxby et al., 2011; Haxby et al., 2020). Other methods developed to address functional alignment include template-matching techniques (e.g., (Gordon et al., 2017a; Gordon et al., 2017b)), multi-modal functional/anatomical registration (Glasser et al., 2016), and hierarchical functional parcellation approaches (e.g., (Kong et al., 2019; Kong et al., 2021)) to identify brain systems and regions in individuals even with more modest amounts of data.

Each of these methods has demonstrated great utility in allowing us to make cross-subject comparisons to investigate various research questions, including improved definition of default systems (Braga and Buckner, 2017; Gilmore et al., 2021; Gordon et al., 2020), language systems (Braga et al., 2020; Fedorenko et al., 2012; 2013), and sensory-biased frontal regions (Noyce et al., 2017; Somers et al., 2021). However, our work here suggests that they must be implemented in such a way that is able to account for not only local displacements (i.e., proximally altered positions due to border shifts) but also more distant deviations caused by ectopic intrusions. Many current approaches rely on adjusting individual functional regions within a relatively restricted spatial extent, and while this is likely appropriate for many brain locations, imposing a strict distance criterion will not be optimized for detecting ectopic variants that are more distant from their typical network boundaries (see Supp. Fig. 3; nearly one-third of all ectopic variants occur at a distance of more than 30 mm from their same-network boundaries).

Adjusting for ectopic variants will be more relevant in some brain locations and functional networks than others. Compared to border shifts, ectopic variants were much more prevalent in lateral frontal cortex, a region believed to play a role in task control (Dosenbach et al., 2006; Duncan and Owen, 2000; Gratton et al., 2018b), language (Fedorenko et al., 2012; 2013), and sensory-biased attention and working memory (Noyce et al., 2017), among other high-level processes. The prevalence of ectopic variants in lateral frontal cortex suggest that researchers should be particularly cautious in interpreting group-level results in these regions, unless a cross-subject functional alignment method is performed that accounts for non-local deviations. Indeed, important advances in our understanding of lateral frontal cortex will likely be spurred by studies using improved functional alignment methods, which enable separation of multifunctional regions from specialized regions in the face of cross-subject heterogeneity (e.g., (Assem et al., 2020; Fedorenko et al., 2012); see review by (Smith et al., 2021)). In contrast, border variants were more commonly localized to the temporoparietal junction and rostral superior frontal regions, which have been linked to shifting attention (Corbetta and Shulman, 2002) and theory of mind (DiNicola et al., 2020; Saxe, 2006; Saxe and Kanwisher, 2003) among other functions, suggesting that studies focusing on these domains and areas may benefit from functional alignment approaches which impose distance-constrained changes.

3.4. Impact for studies of individual differences

One notable difference between the two variant forms is in how they co-vary across participants. In both cases, sub-groups of individuals showed similar patterns of variants: for example, with both forms of variants, one sub-group had variants with strong links to the DMN, while another sub-group had variants with stronger links to top-down control networks. However, the sub-groups differed in their specific variant profiles (e.g., whether the fronto-parietal network was grouped with the DMN or CO subgroup). Perhaps most notably, the two variant forms appeared independent: that is, a person in the "DMN" subgroup based on border variants could easily be in the ectopic subgroup based on ectopic variants. Other forms of individual variation were also seen in variant properties. For example, there was variation in the relative proportion of each variant form across participants (e.g., MSC02 and MSC06 had relatively few ectopic variants, while MSC01 and MSC05 had many; Fig. 1). These findings beg the question of how each form of variation in cortical organization is related to individual differences in cognition and behavior.

In our previous work, we demonstrated that network variants have high stability across sessions, even up to a year (Seitzman et al., 2019) and across task states (Kraus et al., 2021). This trait-like characteristic of network variants, as well as its link to differences in functional responses during tasks ((Seitzman et al., 2019) Fig. 4) suggest that they are well suited to serve as biomarkers of individual differences in behavior in both the neurotypical population (Seitzman et al., 2019) and in cases of psychiatric and neurological disorders (Gratton et al., 2020). Other studies have also shown that individual differences in functional brain organization relate to behavior, including links between individual-level network topography and measures of cognition and emotion (Kong et al., 2019), associations between changes in functional network topography and a variety of behavioral factors (Bijsterbosch et al., 2018), and links between cognitive ability and maturation of networks supporting executive function (Cui et al., 2020; Satterthwaite et al., 2013).

The differences we find between border and ectopic variants suggest that deeper insights into individual differences will be provided if these two forms of variation are separated. This understanding will allow for improved theories about the mechanistic links between individual differences in brain system variation and behavior, likely critical to using this information to guide clinical practice and interventions.

4. CONCLUSION

While the human cortex is organized around a common core architecture, specific locations exhibit prominent deviations from this group-average organization. Here, we investigated two forms of these deviations: nearby shifts in the borders between functional systems and ectopic intrusions at a distance from their typical position. We demonstrate that these two forms of individual variation are both common, but differ in their spatial positions, network associations, task response patterns, and sub-grouping characteristics. These different properties that both forms of variation must be accounted for in the study of cortical system organization and its links to behavior.

5. METHODS

5.1. Datasets and Overview

Network variants were investigated using data from two separate publicly available datasets: the Midnight Scan Club (MSC) dataset (Gordon et al., 2017c), and a subset of individuals from the Human Connectome Project (HCP) (Van Essen et al., 2012b). The MSC dataset is a "precision" fMRI dataset consisting of 10 highly sampled subjects (4 female; average age 29.3 years; 1 participant excluded due to high motion and sleep (Gordon et al., 2017c)) with over 154 minutes of low-motion rest fMRI data and task fMRI data across 3 conditions (mixed, memory, motor - in this manuscript we focus on the results of the mixed design tasks). From the larger HCP dataset, we analyzed 384 unrelated subjects (210 female; average age 28.4 years as in (Seitzman et al., 2019), selected to be unrelated and have a minimum of 45 min. of low motion resting-state fMRI; see SI Table 1 in Seitzman et al., 2019 for details on exclusion criteria for this dataset).

In both datasets, previously defined idiosyncratic locations of functional connectivity ("network variants"; Seitzman et al., 2019) were divided into homogeneous segments (see criteria below) and segregated into ectopic intrusions ("ectopic variants") and border shifts ("border variants") based on the criteria described below. Several features of each variant form were then examined. First, we quantified the prevalence of both variant forms across the two datasets. Second, we characterized the spatial location and idiosyncratic (individual-specific) network assignment of these regions. Third, we examined the task responses of both variant forms using task data from the MSC dataset. Fourth, we examined if there were common profiles of border shift and ectopic variants (as we have seen in past data for variants as a whole; Seitzman et al., 2019), by clustering individuals into sub-groups based on their variant characteristics.

5.2. Preprocessing

Imaging data from the MSC and HCP subjects used in the present analyses were preprocessed identically to Seitzman et al. (2019). Full details on acquisition parameters, preprocessing, FC processing, and volume-to-surface mapping can be found in that manuscript, but are outlined briefly below.

Functional data from both datasets were preprocessed to remove noise and artifacts, following (Miezin et al., 2000). For the HCP dataset, we began with the dataset as processed following the minimal preprocessing pipelines (Glasser et al., 2013). Procedures included field map distortion correction of the functional images, slice-timing correction (for the MSC dataset only), mode-1000 normalization, motion correction via a rigid body transformation, affine registration of functional data to a T1-weighted image, and affine alignment into stereotactic atlas space (MNI for HCP (Montreal Neurological Institute, Montreal, QC, Canada); Talairach for MSC (Talairach and Tournoux, 1988)).

Following this, resting-state fMRI data was further denoised for functional connectivity analysis, including regression of white matter, cerebrospinal fluid, and whole brain signals, six rigid-body parameters and their derivatives, and their expansion terms (Friston et al., 1996). High-motion frames (calculated as framewise displacement; FD (Power et al., 2012)) were censored; frames

with FD > 0.2 were censored for the MSC data (Gordon et al., 2017c) and frames with filtered FD > 0.1 were censored from the HCP data following (Fair et al., 2020) to address respiration contamination of motion parameters (filtered FD = low-pass filtering at <0.1 Hz of the original motion parameters prior to FD calculation; note that two participants in the MSC dataset – MSC03 and MSC10 – with strong respiratory contamination of their motion parameters also used the filtered FD measure (Gordon et al., 2017c; Gratton et al., 2018a). As in (Power et al., 2014), 5 frames at the start of each run along with any segments < 5 frames long were also removed. These censored frames were interpolated over using a power-spectral matched interpolation. Subsequent to this, a temporal bandpass filter was applied to the data from 0.009 to 0.08 Hz.

Following this processing, BOLD data were mapped to each subject's native cortical surface as generated by FreeSurfer from the atlas-registered T1 (Dale et al., 1999). Data were registered into fs_LR space (Van Essen et al., 2012a) and were aligned to the surface following Gordon et al. (2016), producing a CIFTI file with a BOLD timeseries for each functional run.

Data on the cortical surface was spatially smoothed with the application of a geodesic smoothing kernel ($\sigma = 2.55$; FWHM = 6 mm). Finally, high motion frames (that were previously interpolated) were removed from analysis. Note that participants were required to have at least 45 min. of data total to be retained in analysis (see (Kraus et al., 2021; Seitzman et al., 2019) for evidence that ~40 minutes of data is necessary to achieve reliable network variant measures).

5.3. Defining network variants

Network variants are defined as locations in an individual that show strong differences in their functional network patterns relative to the group average. In the current manuscript we began with the same set of variants as originally presented in (Seitzman et al., 2019). Briefly, for each subject, each vertex's seedmap (i.e., its cortex-wide connectivity map) was correlated with the same vertex's seedmap from a group-average reference dataset, composed of an independent 120 young adults (the WashU 120, (Gordon et al., 2017a)). After repeating this procedure for all cortical vertices, this produced one individual:group similarity map per person (with a spatial correlation value for each vertex). Similarity maps were thresholded to include only the lowest decile of correlation values (i.e., to identify the 10% of locations where the individual was least similar from the group-average) and were then binarized. As in (Seitzman et al., 2019), a vertex-wise map of low-signal regions was used to mask out potential variant locations. Clusters of at least 50 neighboring vertices in size were flagged as pre-variants for further analysis (see Supp. Fig. 1A).

Following this original variant definition, a series of steps was taken to further refine the set of pre-variants to generate the final variants that were used in the border/ectopic analyses, given observations that some pre-variants were large and irregularly shaped, suggesting they might consist of separate units. To divide pre-variants, previously defined contiguous units were divided into segments with the goal of minimizing heterogeneity in the connectivity profile of individual pre-variants. This procedure consisted of a two-fold check of (1) the variance explained by the first principal component of the pre-variant, resulting from a principal component analysis on variants' vertex-wise seed maps (i.e., 'homogeneity' (Gordon et al.,

2016)) and (2) the proportion of the variant's territory that is dominated by a single network in the individual's subject-specific vertex-wise network map. In these vertex-wise maps, each cortical vertex is individually assigned to a network using a template-matching procedure (see (Dworetsky et al., 2021; Gordon et al., 2017a; Gordon et al., 2017b) which matches each vertex's thresholded seedmap to each network's thresholded seedmap (each thresholded at the top 5% of values) and assigns the vertex to the network with the best fit (measured via the Dice coefficient; similar to (Gordon et al., 2017b)). Using the MSC as a pilot dataset and manually rating whether each pre-variant should be flagged to be divided based on these criteria, thresholds were set at 66.7% homogeneity and 75% network dominance in the individual network map. If a pre-variant did not exceed both criteria, it was flagged to be divided. Flagged pre-variants were split along the network boundaries of the vertex-wise network, resulting in final "split" variants into homogenous regions. Clusters smaller than 30 contiguous voxels were removed. See Supp. Fig. 1B for a schematic representation of the splitting procedure and examples of split variants.

5.4. Functional network assignment of variants

Variants were then assigned to a best-fitting canonical functional network by a procedure which matched each variant to its best-fitting functional network template as in (Seitzman et al., 2019). To assign variants to networks in the MSC dataset we used group-average network templates that were generated in previous work (Seitzman et al., 2019) from 14 networks using data from the WashU 120 (Gordon et al., 2017b; Seitzman et al., 2019); see Supp. Fig. 5A). Networks used for MSC analyses included default mode (DMN), visual, fronto-parietal (FP), dorsal attention (DAN), language (Lang.; note this has been referred to as the ventral attention network in our past work but we have now reclassified as language based on its correspondence with language localizers (Braga et al., 2020)), salience, cingulo-opercular (CO), somatomotor dorsal (SMd), somatomotor lateral (SMl), auditory, temporal pole (Tpole), medial temporal lobe (MTL), parietal medial (PMN), and parieto-occipital (PON).

For the HCP dataset (given differences in dataset resolution and acquisition parameters (Van Essen et al., 2012b); see also (Dworetsky et al., 2021)), a dataset-specific network template was generated from the set of 384 subjects (Supp. Fig. 5B; see Seitzman et al. (2019) for template generation procedure). The networks included in HCP-specific analyses were similar to those for the MSC, but did not include the language, MTL, or T-pole networks as these networks did not emerge consistently across edge density thresholds from the data-driven group-average network identification procedure (Infomap; (Rosvall and Bergstrom, 2008)). In both cases, the average seedmap for each variant in an individual was compared with each of the network templates (after binarizing both to the top 5% of connectivity values (as in (Gordon et al., 2017b)) and assigned to the template with the highest Dice coefficient overlap. Network variants were removed from further analysis if they did not match to any functional network (Dice coefficient of zero) or if over 50% of their vertices overlapped with the group-average network for that location.

5.5. Classification of variants as ectopic intrusions or border shifts

In order to classify variants as either ectopic intrusions or border shifts, a distance-based algorithm was implemented to identify the variants which lay adjacent or at a distance from the canonical group-average boundaries of the same network. First, using the MSC as a pilot dataset, all variants were manually classified as ectopic variants by examining whether they visually appeared to be spatial extensions of existing network features or whether they appeared to arise unconnected from other same-network locations. Next, an algorithm was produced to optimize agreement of computed border/ectopic classifications with the manual classifications. The final procedure specified that all variants further than 3.5 mm (edge-to-edge distance) away from a same-network cluster were classified as ectopic variants; variants closer than 3.5 mm were classified as border variants. This procedure was then applied to the independent HCP dataset (see Supp. Fig. 1C for schematic representation). As a check to determine whether the 3.5 mm distance threshold we specified would significantly impact the proportion of ectopic variants in our sample, we also classified variants as ectopic or border based on a distance criterion of 5, 7.5, and 10 mm and computed the proportion of ectopic variants at each. Finally, we also quantified the distance between each final ectopic variant and canonical regions of that network.

5.6. Examining differences in spatial distribution between ectopic and border variants

To visualize the spatial distribution of border and ectopic network variants, a spatial overlap map was generated by summing network variant maps (separated by form) across individuals. This produced an overlap map highlighting regions of high and low occurrence of variants.

These spatial overlap maps were quantitatively contrasted at two levels. First, an omnibus map-wise permutation analysis was run. This was achieved by (1) shuffling variant classification labels (ectopic vs. border) within each subject's variants map to create pseudo-ectopic and pseudo-border variants in the same proportion, (2) summing variant locations across subjects to generate a cross-subject overlap map for pseudo-ectopic variants and a cross-subject overlap map for pseudo-border variants, (3) calculating the similarity (spatial correlation) between the pseudo-ectopic and pseudo-border overlap maps, and (4) repeating steps 1-3 1000 times for different permuted labels. We then compared the distribution of permuted similarity values with the true similarity between ectopic and border spatial distribution maps. We calculated significance as a *p*-value based on the proportion of permutations in which the permuted correlation value exceeded the true correlation value. This procedure was used to determine whether spatial distributions, as a whole, differed between ectopic intrusions and border shifts.

Second, to locate specific regions where the distribution of ectopic variants was significantly distinct from border variants, a cluster-size based permutation analysis was run. The first two steps were the same as before: (1) shuffling ectopic and border labels within each subject's variant map to create pseudo-ectopic and pseudo-border variants in the same proportion and (2) summing variant locations across subjects to create an overlap map for pseudo-ectopic and pseudo-border variants. Then, we (3) generated a difference map of the pseudo-ectopic variants distribution minus the pseudo-border variants distribution, (4) thresholded this pseudo-difference map to only keep locations with differences of at least 5% of participants (20 subjects), and (5) calculated the size (number of vertices) of retained clusters. This procedure was repeated 1000 times, producing 1000 permuted pseudo cluster size calculations. This distribution of cluster sizes was used to select a cluster threshold that corresponded to the top 5% of permuted

(random-chance) clusters ($p < 0.05$ cluster-corrected). Final difference values are shown as Z-maps comparing, at each vertex, random-chance distributions with the actual distribution.

5.7. Comparing network assignments between variant forms

In addition to its spatial location, each variant has an idiosyncratic functional network assignment (see "Functional network assignment of variants" section above; e.g., a network variant located in a typical DMN region may have a functional connectivity profile more closely associated with FP, causing it to be assigned to that system). In the next analysis, we used a permutation approach to quantify differences in border and ectopic variants' functional network assignments.

For this analysis: (1) we permuted the label of each variant as border or ectopic within participants in the HCP dataset (permutations were done per participant), (2) we then calculated the proportion of pseudo-ectopic to pseudo-border variants for each network, (3) repeated steps 1-2 1000 times. We then compared the true ectopic to border proportion for each network to the permuted distribution of proportions. Significance was assessed via *p*-values calculated as the proportion of permutations in which a network's true percentage of ectopic variants was less or greater than (two-tailed) all permuted percentages after FDR correcting for multiple comparisons across networks.

Finally, we determined the "swaps" of network territory occupied by border and ectopic variants (e.g., a variant located in canonical cingulo-opercular territory that "swaps" its network assignment to the fronto-parietal network). To do so, we defined each variant's consensus network assignment as the modal network across variant vertices in the pre-defined group-average system map, compared this with the variant's assigned network, and tabulated the frequency of all cross-network swaps.

5.8. Examining task activation profiles of forms of variants

In addition to defining FC features of network variants, we also examined how these regions responded during tasks. Following (Seitzman et al., 2019), we focused on fMRI task activations during the mixed-design tasks in the MSC dataset (semantic and coherence), given strong a-priori hypotheses about the responses of different networks during these tasks. The semantic task involved participants indicating whether presented words were nouns or verbs, and the coherence task required participants to indicate whether an array of white dots on a black background (Glass, 1969) were displayed in a concentric (as opposed to random) arrangement. Within each task block, a short cue signaled the onset of the block, with a series of individual trials presented with jittered timing. Another short cue signaled the end of the block, and task blocks were separated by fixation periods of 44 seconds (see (Gordon et al., 2017c) for more details on task design).

Task fMRI data from the MSC dataset underwent the same basic preprocessing as listed in the *Preprocessing* section (i.e., field map correction, slice timing correction, motion correction, alignment, and normalization, registration to the cortical surface and smoothing). These tasks were then analyzed using a general linear model (GLM). For each event (cues, correct and error

trials of each type), eight separate timepoints were modeled in a finite impulse response modeling approach (Miezin et al., 2000)); for each task block, a block regressor was modeled to estimate sustained activations. The tasks and analysis streams are described in further detail by (Gordon et al., 2017c) and (Gratton et al., 2018a).

In this study, we examined the activation image across all conditions (start/end cues, trials, and sustained activations across semantic and coherence tasks) versus baseline to interrogate network variant locations to examine whether forms of variants exhibited differences in task activations. A series of comparisons were conducted following (Seitzman et al., 2019): (1) a comparison of the task activation of DMN variant locations in a given subject relative to the same location in other subjects, (2) a comparison of task activations of variant locations in each network relative to their canonical network locations, and (3) a comparison of task activations of variant locations in each network relative to other networks' canonical locations. Task activations were examined separately for ectopic variants and border variants.

5.9. Identifying sub-groups of ectopic and border variants across individuals

We next sought to investigate whether there were commonalities across sub-groups of individuals in their network variant characteristics. To this end, we conducted a similar analysis as in (Seitzman et al., 2019) to examine the sub-grouping potential of ectopic and border variants.

As in (Seitzman et al., 2019), we split the HCP dataset into 2 matched samples consisting of 192 subjects each, allowing us to search for data-driven findings that replicate across split-halves. In every individual in the HCP dataset, the mean similarity of all variants (calculated per variant vertex) was calculated to each template network using correlation. This created an 11 x 1 vector for each subject containing information on the network similarity profile of variant locations. These average profiles were correlated between all subjects in each split half, producing a 192 x 192 matrix. A data-driven approach, the Infomap clustering algorithm (Rosvall and Bergstrom, 2008), was then conducted on the 192 x 192 cross-subject correlation matrix; the algorithm was applied after thresholding the correlation matrix across a wide range of density thresholds (5% to 50%, in increments of 1%). Sub-groups were defined based on consistent results across a range of Infomap thresholds. Here, three primary sub-groups were consistently produced across a broad range of thresholds (34% and higher for border variants; 29% and higher for ectopic variants); also note that additional sub-groups can be identified at sparser thresholds). Sub-groups of individuals with similar network similarity profiles were identified in the first (discovery) split-half, and the sub-groups were replicated in the second (validation) split-half. Variant network connectivity patterns of resulting sub-groups of individuals were subsequently examined. The sub-grouping analysis was performed twofold: first operating solely on ectopic variants, then operating solely on border variants.

Finally, we examined to what extent an individual's sub-group assignment was consistent when grouped by all of their variants, their border variants only, and their ectopic variants only. All HCP subjects with at least one of each form of network variant were included in this analysis. The network profiles of two previously identified stable sub-groups (a DMN sub-group and a control/processing sub-group) were used as templates with which each individual's network

variant profiles were correlated. Similar network profiles were found in original analyses based on all variants (Seitzman et al., 2019); see Supp. Fig. 9 for DMN and control/processing profiles. Following these "forced" sub-groupings, the adjusted Rand index was calculated three-fold to investigate any similarity between an individual's sub-group assignment between (1) all variants and border variants only, (2) all variants and ectopic variants only, and (3) border variants and ectopic variants.

REFERENCES

Anderson, K.M., Ge, T., Kong, R., Patrick, L.M., Spreng, R.N., Sabuncu, M.R., Yeo, B.T.T., and Holmes, A.J. (2021). Heritability of individualized cortical network topography. Proc Natl Acad Sci U S A *118*. 10.1073/pnas.2016271118.

Arcaro, M.J., Schade, P.F., Vincent, J.L., Ponce, C.R., and Livingstone, M.S. (2017). Seeing faces is necessary for face-domain formation. Nat Neurosci *20*, 1404-1412. 10.1038/nn.4635.

Assem, M., Glasser, M.F., Van Essen, D.C., and Duncan, J. (2020). A Domain-General Cognitive Core Defined in Multimodally Parcellated Human Cortex. Cereb Cortex *30*, 4361-4380. 10.1093/cercor/bhaa023.

Bijsterbosch, J.D., Woolrich, M.W., Glasser, M.F., Robinson, E.C., Beckmann, C.F., Van Essen, D.C., Harrison, S.J., and Smith, S.M. (2018). The relationship between spatial configuration and functional connectivity of brain regions. Elife *7*. 10.7554/eLife.32992.

Braga, R.M., and Buckner, R.L. (2017). Parallel Interdigitated Distributed Networks within the Individual Estimated by Intrinsic Functional Connectivity. Neuron *95*, 457-471 e455. 10.1016/j.neuron.2017.06.038.

Braga, R.M., DiNicola, L.M., Becker, H.C., and Buckner, R.L. (2020). Situating the left-lateralized language network in the broader organization of multiple specialized large-scale distributed networks. J Neurophysiol *124*, 1415-1448. 10.1152/jn.00753.2019.

Brennan, B.P., Wang, D., Li, M., Perriello, C., Ren, J., Elias, J.A., Van Kirk, N.P., Krompinger, J.W., Pope, H.G., Jr., Haber, S.N., et al. (2019). Use of an Individual-Level Approach to Identify Cortical Connectivity Biomarkers in Obsessive-Compulsive Disorder. Biol Psychiatry Cogn Neurosci Neuroimaging *4*, 27-38. 10.1016/j.bpsc.2018.07.014.

Cadwell, C.R., Bhaduri, A., Mostajo-Radji, M.A., Keefe, M.G., and Nowakowski, T.J. (2019). Development and Arealization of the Cerebral Cortex. Neuron *103*, 980-1004. 10.1016/j.neuron.2019.07.009.

Churchland, P.S., and Sejnowski, T.J. (1988). Perspectives on cognitive neuroscience. Science *242*, 741-745. 10.1126/science.3055294.

Corbetta, M., and Shulman, G.L. (2002). Control of goal-directed and stimulus-driven attention in the brain. Nat Rev Neurosci *3*, 201-215. 10.1038/nrn755.

Cui, Z., Li, H., Xia, C.H., Larsen, B., Adebimpe, A., Baum, G.L., Cieslak, M., Gur, R.E., Gur, R.C., Moore, T.M., et al. (2020). Individual Variation in Functional Topography of Association Networks in Youth. Neuron *106*, 340-353 e348. 10.1016/j.neuron.2020.01.029.

Dale, A.M., Fischl, B., and Sereno, M.I. (1999). Cortical surface-based analysis. I. Segmentation and surface reconstruction. Neuroimage *9*, 179-194. 10.1006/nimg.1998.0395.

DiNicola, L.M., Braga, R.M., and Buckner, R.L. (2020). Parallel distributed networks dissociate episodic and social functions within the individual. J Neurophysiol *123*, 1144-1179. 10.1152/jn.00529.2019.

DiNicola, L.M., and Buckner, R.L. (2021). Precision Estimates of Parallel Distributed Association Networks: Evidence for Domain Specialization and Implications for Evolution and Development. Curr Opin Behav Sci *40*, 120-129. 10.1016/j.cobeha.2021.03.029.

Dosenbach, N.U., Visscher, K.M., Palmer, E.D., Miezin, F.M., Wenger, K.K., Kang, H.C., Burgund, E.D., Grimes, A.L., Schlaggar, B.L., and Petersen, S.E. (2006). A core system for the implementation of task sets. Neuron *50*, 799-812. 10.1016/j.neuron.2006.04.031.

Dougherty, R.F., Koch, V.M., Brewer, A.A., Fischer, B., Modersitzki, J., and Wandell, B.A. (2003). Visual field representations and locations of visual areas V1/2/3 in human visual cortex. J Vis *3*, 586-598. 10.1167/3.10.1.

Duncan, J., and Owen, A.M. (2000). Common regions of the human frontal lobe recruited by diverse cognitive demands. Trends Neurosci *23*, 475-483. 10.1016/s0166-2236(00)01633-7.

Dworetsky, A., Seitzman, B.A., Adeyemo, B., Neta, M., Coalson, R.S., Petersen, S.E., and Gratton, C. (2021). Probabilistic mapping of human functional brain networks identifies regions of high group consensus. Neuroimage *237*, 118164. 10.1016/j.neuroimage.2021.118164.

Eickhoff, S.B., Yeo, B.T.T., and Genon, S. (2018). Imaging-based parcellations of the human brain. Nat Rev Neurosci *19*, 672-686. 10.1038/s41583-018-0071-7.

Fair, D.A., Miranda-Dominguez, O., Snyder, A.Z., Perrone, A., Earl, E.A., Van, A.N., Koller, J.M., Feczko, E., Tisdall, M.D., van der Kouwe, A., et al. (2020). Correction of respiratory artifacts in MRI head motion estimates. Neuroimage *208*, 116400. 10.1016/j.neuroimage.2019.116400.

Fan, Y.S., Li, L., Peng, Y., Li, H., Guo, J., Li, M., Yang, S., Yao, M., Zhao, J., Liu, H., et al. (2020). Individual-specific functional connectome biomarkers predict schizophrenia positive symptoms during adolescent brain maturation. Hum Brain Mapp. 10.1002/hbm.25307.

Fedorenko, E. (2021). The early origins and the growing popularity of the individual-subject analytic approach in human neuroscience. Current Opinion in Behavioral Sciences *40*, 105-112. 10.1016/j.cobeha.2021.02.023.

Fedorenko, E., and Blank, I.A. (2020). Broca's Area Is Not a Natural Kind. Trends Cogn Sci *24*, 270-284. 10.1016/j.tics.2020.01.001.

Fedorenko, E., Duncan, J., and Kanwisher, N. (2012). Language-selective and domain-general regions lie side by side within Broca's area. Curr Biol *22*, 2059-2062. 10.1016/j.cub.2012.09.011.

Fedorenko, E., Duncan, J., and Kanwisher, N. (2013). Broad domain generality in focal regions of frontal and parietal cortex. Proc Natl Acad Sci U S A *110*, 16616-16621. 10.1073/pnas.1315235110.

Finn, E.S., Shen, X., Scheinost, D., Rosenberg, M.D., Huang, J., Chun, M.M., Papademetris, X., and Constable, R.T. (2015). Functional connectome fingerprinting: identifying individuals using patterns of brain connectivity. Nat Neurosci *18*, 1664-1671. 10.1038/nn.4135.

Fischl, B. (2012). FreeSurfer. Neuroimage *62*, 774-781. 10.1016/j.neuroimage.2012.01.021.

Friston, K.J., Williams, S., Howard, R., Frackowiak, R.S., and Turner, R. (1996). Movement-related effects in fMRI time-series. Magn Reson Med *35*, 346-355. 10.1002/mrm.1910350312.

Frost, M.A., and Goebel, R. (2012). Measuring structural-functional correspondence: spatial variability of specialised brain regions after macro-anatomical alignment. Neuroimage *59*, 1369-1381. 10.1016/j.neuroimage.2011.08.035.

Gilmore, A.W., Nelson, S.M., and McDermott, K.B. (2021). Precision functional mapping of human memory systems. Current Opinion in Behavioral Sciences *40*, 52-57. 10.1016/j.cobeha.2020.12.013.

Glass, L. (1969). Moire effect from random dots. Nature *223*, 578-580. 10.1038/223578a0.

Glasser, M.F., Coalson, T.S., Robinson, E.C., Hacker, C.D., Harwell, J., Yacoub, E., Ugurbil, K., Andersson, J., Beckmann, C.F., Jenkinson, M., et al. (2016). A multi-modal parcellation of human cerebral cortex. Nature *536*, 171-178. 10.1038/nature18933.

Glasser, M.F., Sotiropoulos, S.N., Wilson, J.A., Coalson, T.S., Fischl, B., Andersson, J.L., Xu, J., Jbabdi, S., Webster, M., Polimeni, J.R., et al. (2013). The minimal preprocessing pipelines for the Human Connectome Project. Neuroimage *80*, 105-124. 10.1016/j.neuroimage.2013.04.127.

Gordon, E.M., Laumann, T.O., Adeyemo, B., Gilmore, A.W., Nelson, S.M., Dosenbach, N.U.F., and Petersen, S.E. (2017a). Individual-specific features of brain systems identified with resting state functional correlations. Neuroimage *146*, 918-939. 10.1016/j.neuroimage.2016.08.032.

Gordon, E.M., Laumann, T.O., Adeyemo, B., Huckins, J.F., Kelley, W.M., and Petersen, S.E. (2016). Generation and Evaluation of a Cortical Area Parcellation from Resting-State Correlations. Cereb Cortex *26*, 288-303. 10.1093/cercor/bhu239.

Gordon, E.M., Laumann, T.O., Adeyemo, B., and Petersen, S.E. (2017b). Individual Variability of the System-Level Organization of the Human Brain. Cereb Cortex *27*, 386-399. 10.1093/cercor/bhv239.

Gordon, E.M., Laumann, T.O., Gilmore, A.W., Newbold, D.J., Greene, D.J., Berg, J.J., Ortega, M., Hoyt-Drazen, C., Gratton, C., Sun, H., et al. (2017c). Precision Functional Mapping of Individual Human Brains. Neuron *95*, 791-807 e797. 10.1016/j.neuron.2017.07.011.

Gordon, E.M., Laumann, T.O., Marek, S., Raut, R.V., Gratton, C., Newbold, D.J., Greene, D.J., Coalson, R.S., Snyder, A.Z., Schlaggar, B.L., et al. (2020). Default-mode network streams for coupling to language and control systems. Proc Natl Acad Sci U S A *117*, 17308-17319. 10.1073/pnas.2005238117.

Gordon, E.M., and Nelson, S.M. (2021). Three types of individual variation in brain networks revealed by single-subject functional connectivity analyses. Current Opinion in Behavioral Sciences *40*, 79-86. 10.1016/j.cobeha.2021.02.014.

Gratton, C., Kraus, B.T., Greene, D.J., Gordon, E.M., Laumann, T.O., Nelson, S.M., Dosenbach, N.U.F., and Petersen, S.E. (2020). Defining Individual-Specific Functional Neuroanatomy for Precision Psychiatry. Biol Psychiatry *88*, 28-39. 10.1016/j.biopsych.2019.10.026.

Gratton, C., Laumann, T.O., Nielsen, A.N., Greene, D.J., Gordon, E.M., Gilmore, A.W., Nelson, S.M., Coalson, R.S., Snyder, A.Z., Schlaggar, B.L., et al. (2018a). Functional Brain Networks Are Dominated by Stable Group and Individual Factors, Not Cognitive or Daily Variation. Neuron *98*, 439-452 e435. 10.1016/j.neuron.2018.03.035.

Gratton, C., Sun, H., and Petersen, S.E. (2018b). Control networks and hubs. Psychophysiology *55*. 10.1111/psyp.13032.

Guntupalli, J.S., Feilong, M., and Haxby, J.V. (2018). A computational model of shared fine-scale structure in the human connectome. PLoS Comput Biol *14*, e1006120. 10.1371/journal.pcbi.1006120.

Hahamy, A., Macdonald, S.N., van den Heiligenberg, F., Kieliba, P., Emir, U., Malach, R., Johansen-Berg, H., Brugger, P., Culham, J.C., and Makin, T.R. (2017). Representation of Multiple Body Parts in the Missing-Hand Territory of Congenital One-Handers. Curr Biol *27*, 1350-1355. 10.1016/j.cub.2017.03.053.

Haxby, J.V., Guntupalli, J.S., Connolly, A.C., Halchenko, Y.O., Conroy, B.R., Gobbini, M.I., Hanke, M., and Ramadge, P.J. (2011). A common, high-dimensional model of the representational space in human ventral temporal cortex. Neuron *72*, 404-416. 10.1016/j.neuron.2011.08.026.

Haxby, J.V., Guntupalli, J.S., Nastase, S.A., and Feilong, M. (2020). Hyperalignment: Modeling shared information encoded in idiosyncratic cortical topographies. Elife *9*. 10.7554/eLife.56601.

Juch, H., Zimine, I., Seghier, M.L., Lazeyras, F., and Fasel, J.H. (2005). Anatomical variability of the lateral frontal lobe surface: implication for intersubject variability in language neuroimaging. Neuroimage *24*, 504-514. 10.1016/j.neuroimage.2004.08.037.

Kaas, J.H. (2012). The evolution of neocortex in primates. Prog Brain Res *195*, 91-102. 10.1016/B978-0-444-53860-4.00005-2.

Kanwisher, N., McDermott, J., and Chun, M.M. (1997). The fusiform face area: a module in human extrastriate cortex specialized for face perception. J Neurosci *17*, 4302-4311.

Klein, A., Ghosh, S.S., Avants, B., Yeo, B.T., Fischl, B., Ardekani, B., Gee, J.C., Mann, J.J., and Parsey, R.V. (2010). Evaluation of volume-based and surface-based brain image registration methods. Neuroimage *51*, 214-220. 10.1016/j.neuroimage.2010.01.091.

Kong, R., Li, J., Orban, C., Sabuncu, M.R., Liu, H., Schaefer, A., Sun, N., Zuo, X.N., Holmes, A.J., Eickhoff, S.B., and Yeo, B.T.T. (2019). Spatial Topography of Individual-Specific Cortical Networks Predicts Human Cognition, Personality, and Emotion. Cereb Cortex *29*, 2533-2551. 10.1093/cercor/bhy123.

Kong, R., Yang, Q., Gordon, E., Xue, A., Yan, X., Orban, C., Zuo, X.N., Spreng, N., Ge, T., Holmes, A., et al. (2021). Individual-Specific Areal-Level Parcellations Improve Functional Connectivity Prediction of Behavior. Cereb Cortex. 10.1093/cercor/bhab101.

Kraus, B.T., Perez, D., Ladwig, Z., Seitzman, B.A., Dworetsky, A., Petersen, S.E., and Gratton, C. (2021). Network variants are similar between task and rest states. Neuroimage *229*, 117743. 10.1016/j.neuroimage.2021.117743.

Krubitzer, L.A., and Prescott, T.J. (2018). The Combinatorial Creature: Cortical Phenotypes within and across Lifetimes. Trends Neurosci *41*, 744-762. 10.1016/j.tins.2018.08.002.

Krubitzer, L.A., and Seelke, A.M. (2012). Cortical evolution in mammals: the bane and beauty of phenotypic variability. Proc Natl Acad Sci U S A *109 Suppl 1*, 10647-10654. 10.1073/pnas.1201891109.

Laumann, T.O., Gordon, E.M., Adeyemo, B., Snyder, A.Z., Joo, S.J., Chen, M.Y., Gilmore, A.W., McDermott, K.B., Nelson, S.M., Dosenbach, N.U., et al. (2015). Functional System and Areal Organization of a Highly Sampled Individual Human Brain. Neuron *87*, 657-670. 10.1016/j.neuron.2015.06.037.

Marek, S., Tervo-Clemmens, B., Nielsen, A.N., Wheelock, M.D., Miller, R.L., Laumann, T.O., Earl, E., Foran, W.W., Cordova, M., Doyle, O., et al. (2019). Identifying reproducible individual differences in childhood functional brain networks: An ABCD study. Dev Cogn Neurosci *40*, 100706. 10.1016/j.dcn.2019.100706.

Miezin, F.M., Maccotta, L., Ollinger, J.M., Petersen, S.E., and Buckner, R.L. (2000). Characterizing the hemodynamic response: effects of presentation rate, sampling procedure, and the possibility of ordering brain activity based on relative timing. Neuroimage *11*, 735-759. 10.1006/nimg.2000.0568.

Miller, J.A., D'Esposito, M., and Weiner, K.S. (2021). Using Tertiary Sulci to Map the "Cognitive Globe" of Prefrontal Cortex. J Cogn Neurosci *33*, 1698-1715. 10.1162/jocn_a_01696.

Miranda-Dominguez, O., Mills, B.D., Carpenter, S.D., Grant, K.A., Kroenke, C.D., Nigg, J.T., and Fair, D.A. (2014). Connectotyping: model based fingerprinting of the functional connectome. PLoS One *9*, e111048. 10.1371/journal.pone.0111048.

Mueller, S., Wang, D., Fox, M.D., Yeo, B.T., Sepulcre, J., Sabuncu, M.R., Shafee, R., Lu, J., and Liu, H. (2013). Individual variability in functional connectivity architecture of the human brain. Neuron *77*, 586-595. 10.1016/j.neuron.2012.12.028.

Nieto-Castanon, A., and Fedorenko, E. (2012). Subject-specific functional localizers increase sensitivity and functional resolution of multi-subject analyses. Neuroimage *63*, 1646-1669. 10.1016/j.neuroimage.2012.06.065.

Noyce, A.L., Cestero, N., Michalka, S.W., Shinn-Cunningham, B.G., and Somers, D.C. (2017). Sensory-Biased and Multiple-Demand Processing in Human Lateral Frontal Cortex. J Neurosci *37*, 8755-8766. 10.1523/JNEUROSCI.0660-17.2017.

O'Leary, D.D., Chou, S.J., and Sahara, S. (2007). Area patterning of the mammalian cortex. Neuron *56*, 252-269. 10.1016/j.neuron.2007.10.010.

Porter, A., Nielsen, A., and Gratton, C. (2021). Masked features of task states found in individual brain networks. bioRxiv. 10.1101/2021.06.12.448198.

Power, J.D., Barnes, K.A., Snyder, A.Z., Schlaggar, B.L., and Petersen, S.E. (2012). Spurious but systematic correlations in functional connectivity MRI networks arise from subject motion. Neuroimage *59*, 2142-2154. 10.1016/j.neuroimage.2011.10.018.

Power, J.D., Cohen, A.L., Nelson, S.M., Wig, G.S., Barnes, K.A., Church, J.A., Vogel, A.C., Laumann, T.O., Miezin, F.M., Schlaggar, B.L., and Petersen, S.E. (2011). Functional network organization of the human brain. Neuron *72*, 665-678. 10.1016/j.neuron.2011.09.006.

Power, J.D., Mitra, A., Laumann, T.O., Snyder, A.Z., Schlaggar, B.L., and Petersen, S.E. (2014). Methods to detect, characterize, and remove motion artifact in resting state fMRI. Neuroimage *84*, 320-341. 10.1016/j.neuroimage.2013.08.048.

Rosvall, M., and Bergstrom, C.T. (2008). Maps of random walks on complex networks reveal community structure. Proc Natl Acad Sci U S A *105*, 1118-1123. 10.1073/pnas.0706851105.

Satterthwaite, T.D., Wolf, D.H., Erus, G., Ruparel, K., Elliott, M.A., Gennatas, E.D., Hopson, R., Jackson, C., Prabhakaran, K., Bilker, W.B., et al. (2013). Functional maturation of the executive system during adolescence. J Neurosci *33*, 16249-16261. 10.1523/JNEUROSCI.2345-13.2013.

Saxe, R. (2006). Uniquely human social cognition. Curr Opin Neurobiol *16*, 235-239. 10.1016/j.conb.2006.03.001.

Saxe, R., Brett, M., and Kanwisher, N. (2006). Divide and conquer: a defense of functional localizers. Neuroimage *30*, 1088-1096; discussion 1097-1089. 10.1016/j.neuroimage.2005.12.062.

Saxe, R., and Kanwisher, N. (2003). People thinking about thinking people. The role of the temporo-parietal junction in "theory of mind". Neuroimage *19*, 1835-1842. 10.1016/s1053-8119(03)00230-1.

Schwarzkopf, D.S., Song, C., and Rees, G. (2011). The surface area of human V1 predicts the subjective experience of object size. Nat Neurosci *14*, 28-30. 10.1038/nn.2706.

Seitzman, B.A., Gratton, C., Laumann, T.O., Gordon, E.M., Adeyemo, B., Dworetsky, A., Kraus, B.T., Gilmore, A.W., Berg, J.J., Ortega, M., et al. (2019). Trait-like variants in human functional brain networks. Proc Natl Acad Sci U S A *116*, 22851-22861. 10.1073/pnas.1902932116.

Smith, D.M., Perez, D.C., Porter, A., Dworetsky, A., and Gratton, C. (2021). Light through the fog: using precision fMRI data to disentangle the neural substrates of cognitive control. Current Opinion in Behavioral Sciences *40*, 19-26. 10.1016/j.cobeha.2020.12.004.

Smith, S.M., Nichols, T.E., Vidaurre, D., Winkler, A.M., Behrens, T.E., Glasser, M.F., Ugurbil, K., Barch, D.M., Van Essen, D.C., and Miller, K.L. (2015). A positive-negative mode of population covariation links brain connectivity, demographics and behavior. Nat Neurosci *18*, 1565-1567. 10.1038/nn.4125.

Somers, D.C., Michalka, S.W., Tobyne, S.M., and Noyce, A.L. (2021). Individual subject approaches to mapping sensory-biased and multiple-demand regions in human frontal cortex. Current Opinion in Behavioral Sciences *40*, 169-177. 10.1016/j.cobeha.2021.05.002.

Striem-Amit, E., Ovadia-Caro, S., Caramazza, A., Margulies, D.S., Villringer, A., and Amedi, A. (2015). Functional connectivity of visual cortex in the blind follows retinotopic organization principles. Brain *138*, 1679-1695. 10.1093/brain/awv083.

Tahmasebi, A.M., Davis, M.H., Wild, C.J., Rodd, J.M., Hakyemez, H., Abolmaesumi, P., and Johnsrude, I.S. (2012). Is the link between anatomical structure and function equally strong at all cognitive levels of processing? Cereb Cortex *22*, 1593-1603. 10.1093/cercor/bhr205.

Talairach, J., and Tournoux, P. (1988). Co-planar stereotaxic atlas of the human brain : 3-dimensional proportional system : an approach to cerebral imaging (Georg Thieme).

Van Essen, D.C. (2005). A Population-Average, Landmark- and Surface-based (PALS) atlas of human cerebral cortex. Neuroimage *28*, 635-662. 10.1016/j.neuroimage.2005.06.058.

Van Essen, D.C., Glasser, M.F., Dierker, D.L., Harwell, J., and Coalson, T. (2012a). Parcellations and hemispheric asymmetries of human cerebral cortex analyzed on surface-based atlases. Cereb Cortex *22*, 2241-2262. 10.1093/cercor/bhr291.

Van Essen, D.C., Ugurbil, K., Auerbach, E., Barch, D., Behrens, T.E., Bucholz, R., Chang, A., Chen, L., Corbetta, M., Curtiss, S.W., et al. (2012b). The Human Connectome Project: a data acquisition perspective. Neuroimage *62*, 2222-2231. 10.1016/j.neuroimage.2012.02.018.

Verghese, A., Kolbe, S.C., Anderson, A.J., Egan, G.F., and Vidyasagar, T.R. (2014). Functional size of human visual area V1: a neural correlate of top-down attention. Neuroimage *93 Pt 1*, 47-52. 10.1016/j.neuroimage.2014.02.023.

Wig, G.S., Laumann, T.O., and Petersen, S.E. (2014). An approach for parcellating human cortical areas using resting-state correlations. Neuroimage *93 Pt 2*, 276-291. 10.1016/j.neuroimage.2013.07.035.

Yeo, B.T., Krienen, F.M., Sepulcre, J., Sabuncu, M.R., Lashkari, D., Hollinshead, M., Roffman, J.L., Smoller, J.W., Zollei, L., Polimeni, J.R., et al. (2011). The organization of the human cerebral cortex estimated by intrinsic functional connectivity. J Neurophysiol *106*, 1125-1165. 10.1152/jn.00338.2011.

SUPPLEMENTARY MATERIALS

SUPPLEMENTAL FIGURES

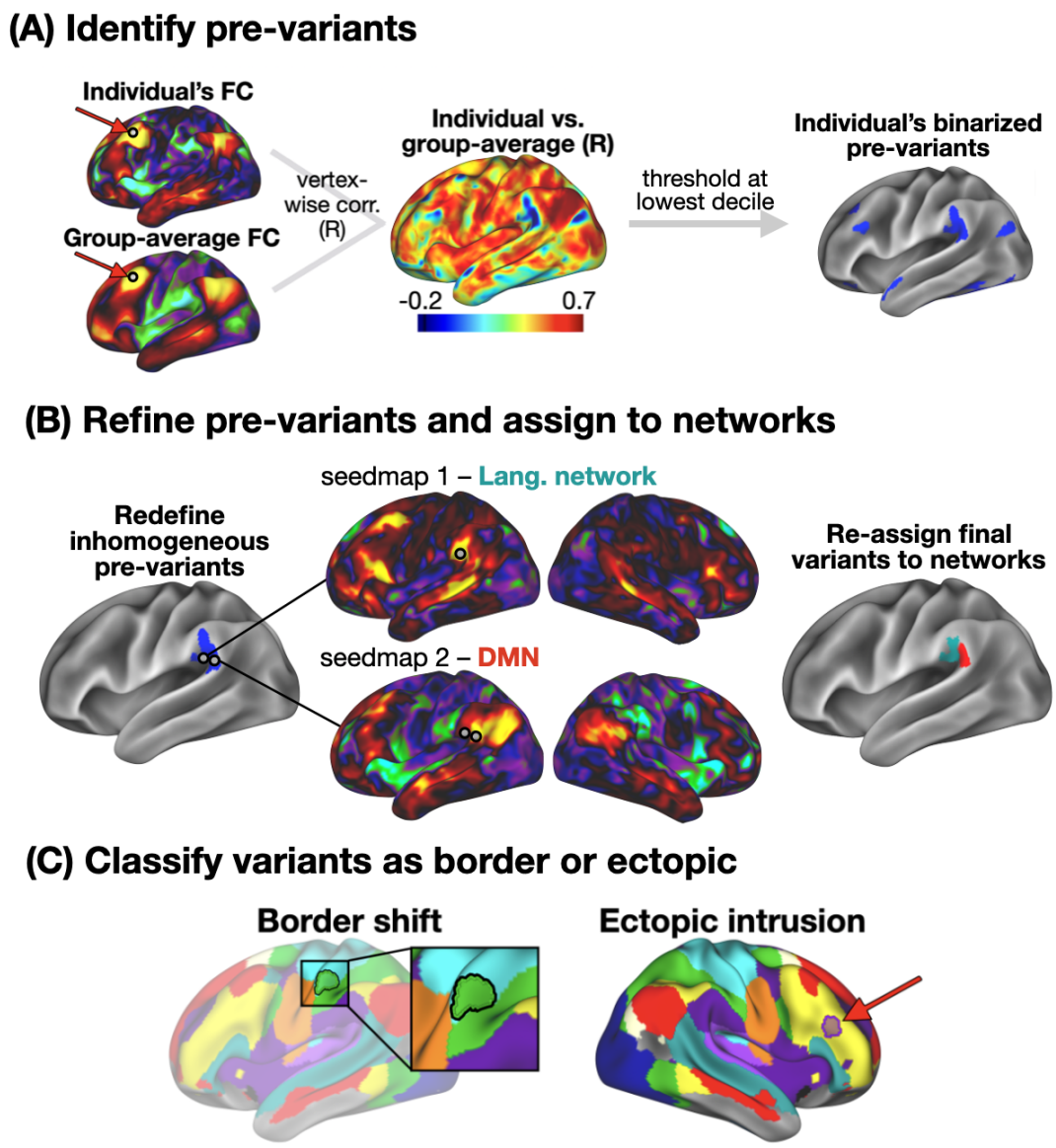

Supp. Fig. 1: Variant definition, splitting, and classification as border or ectopic. (A) Following Seitzman et al., 2019, we used spatial correlation to compare the seedmap at a given location between an individual and an independent group average (left) to generate a individual-to-group "similarity map" (middle). This similarity map was thresholded and binarized to identify locations with low similarity to the group (right) that we call "pre-variants" in this work (Note: these were also thresholded to remove small areas and areas of low signal - see *Methods*). (B) We then further refined these pre-variants to create homogenous units for border vs. ectopic variant classification. Pre-variants were flagged to be divided if either of two criteria indicated high heterogeneity (a PCA "homogeneity" measure (Gordon et al., 2016)) and a measure of

network territory in the subject's network map - see *Methods*). For example, the pre-variant in this panel included two sub-regions, one with relatively high affiliation to the DMN and one with high affiliation to the language network. Flagged pre-variants were then divided along their network map sub-divisions, resulting in a set of final variants for each subject. (C) Finally, each variant was classified as either a border shift or an ectopic intrusion based on its edge-to-edge distance from the nearest same-network boundary in the group-average network map (distances > 3.5 mm were classified as ectopic; distances < 3.5 mm were classified as border; see Fig. 1B and Supp. Fig. 4 for exploration of additional distance criteria).

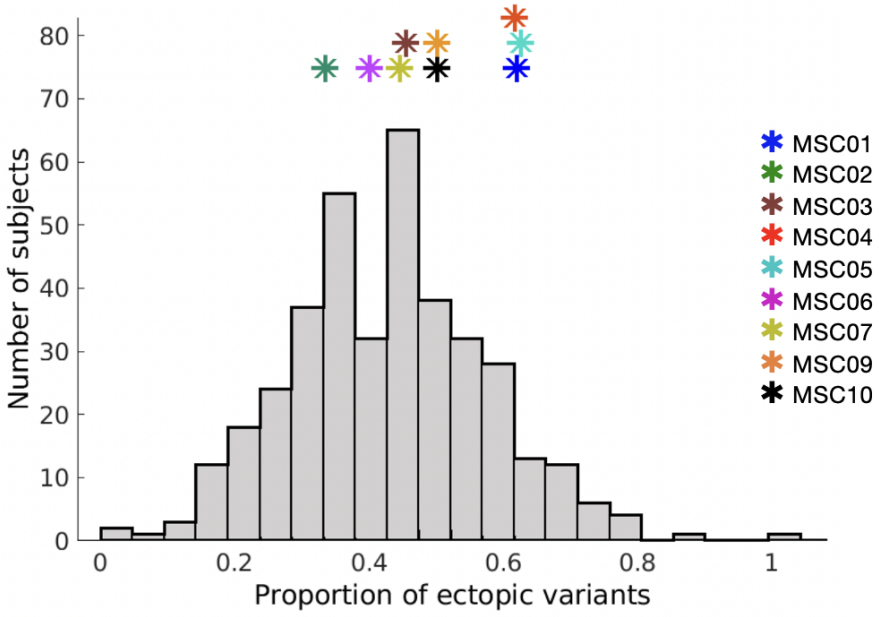

Supp. Fig. 2: Proportion of ectopic variants across subjects. The histogram shows the proportion of ectopic variants (out of total variants) across all subjects in the HCP dataset. Stars on top show the proportion of ectopic variants for each subject in the MSC dataset (labeled at right).

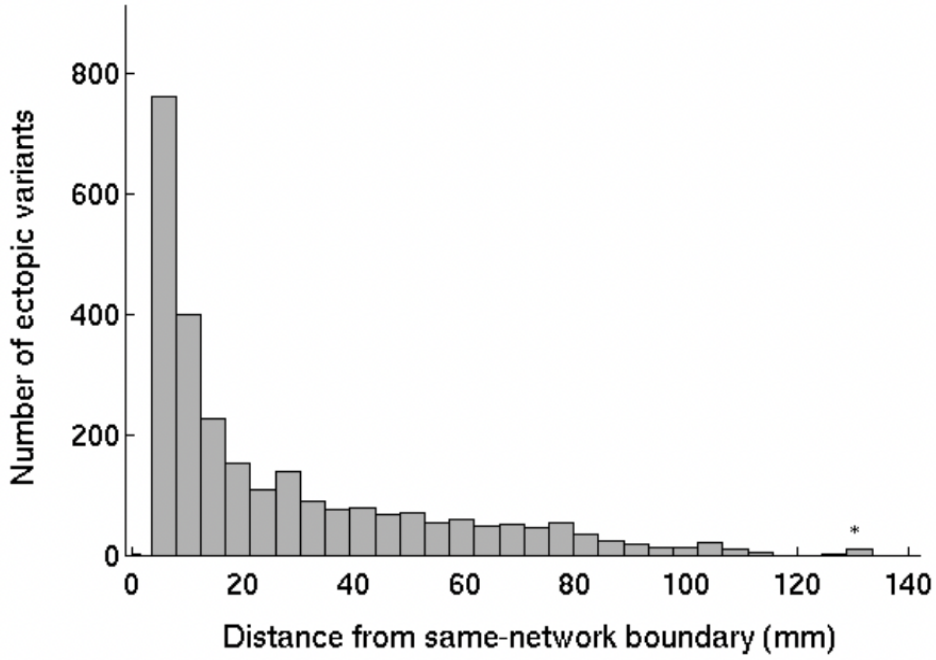

Supp. Fig. 3: Histogram of ectopic variants' distances from their nearest same-network boundary. The plot depicts a histogram of the edge-to-edge distance between each variant and canonical regions of a given network in the HCP dataset. A sizable proportion of ectopic variants are found at a long cortical distance for consensus locations of their network (Median = 15.5 mm; N = 2622 variants).

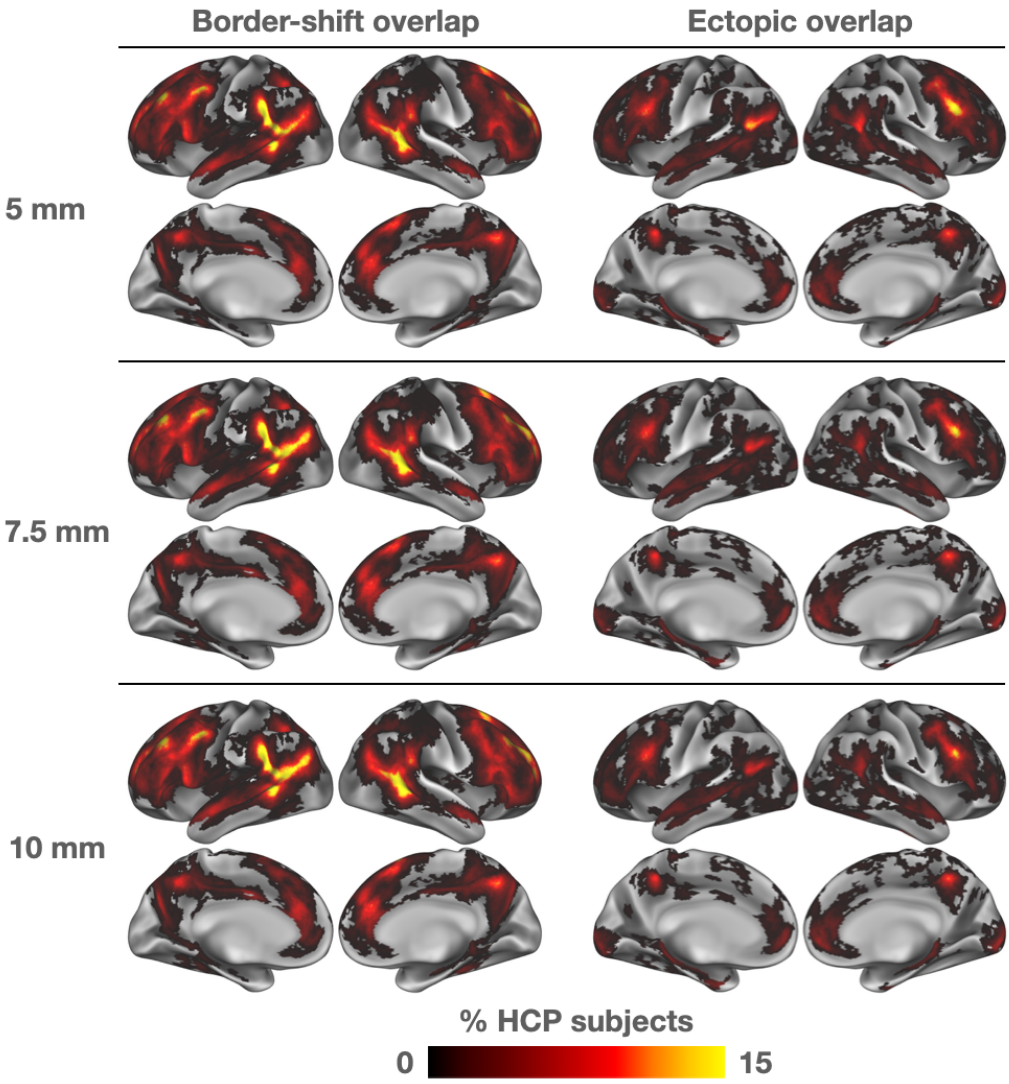

Supp. Fig. 4: Properties of ectopic variants as a function of increasing distance requirement for classification. The spatial distribution patterns observed when ectopic variants in the HCP dataset are defined at > 3.5 mm from network borders (i.e., Fig. 1A in the main manuscript) are largely conserved even as ectopic variant distance is increased through 10 mm.

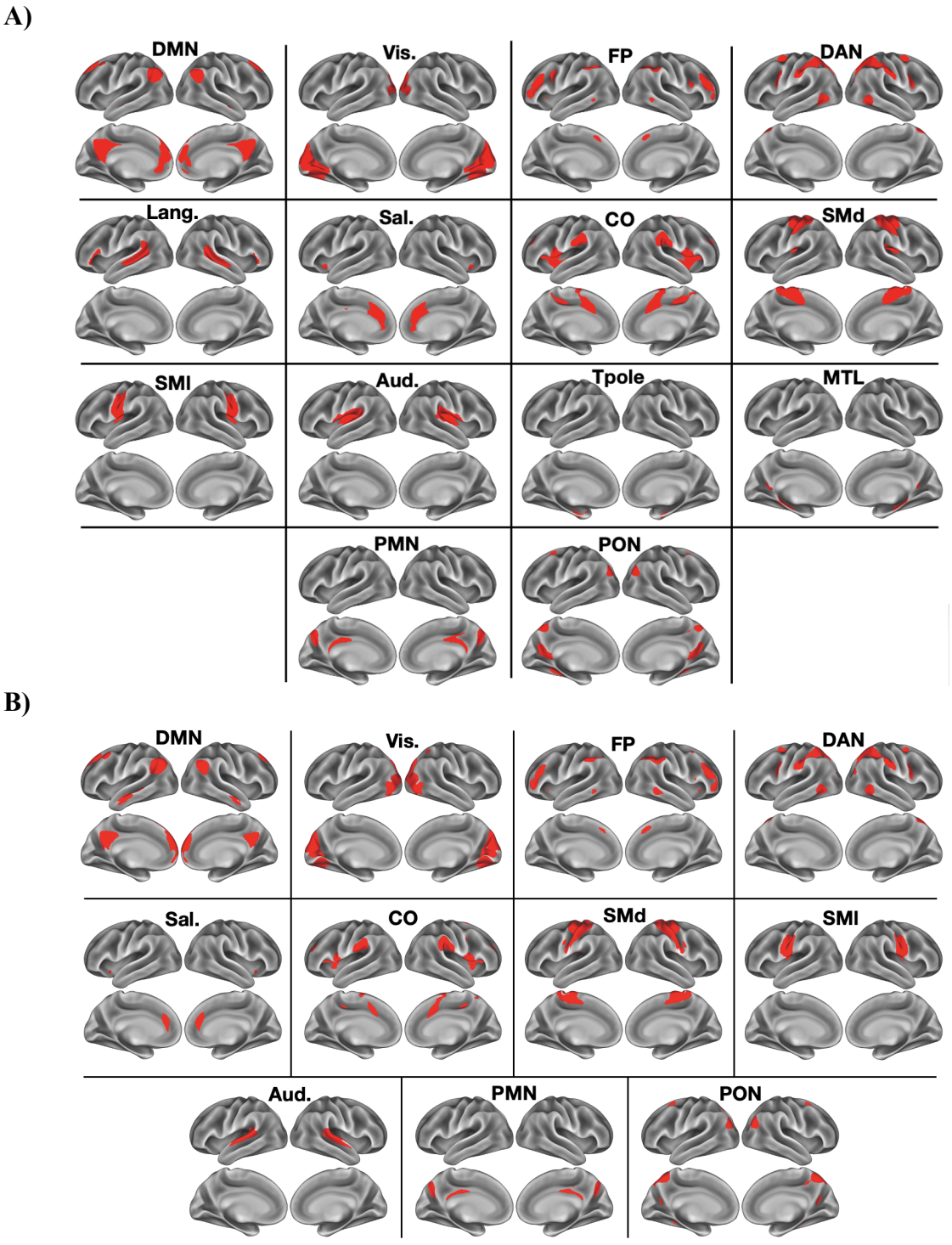

Supp. Fig. 5: Network templates. (A) Network templates derived from the WashU-120 dataset (used for MSC analyses). (B) Network templates derived from the HCP dataset (used for HCP analyses). See *Methods* and (Seitzman et al., 2019) for further details on the generation of network templates.

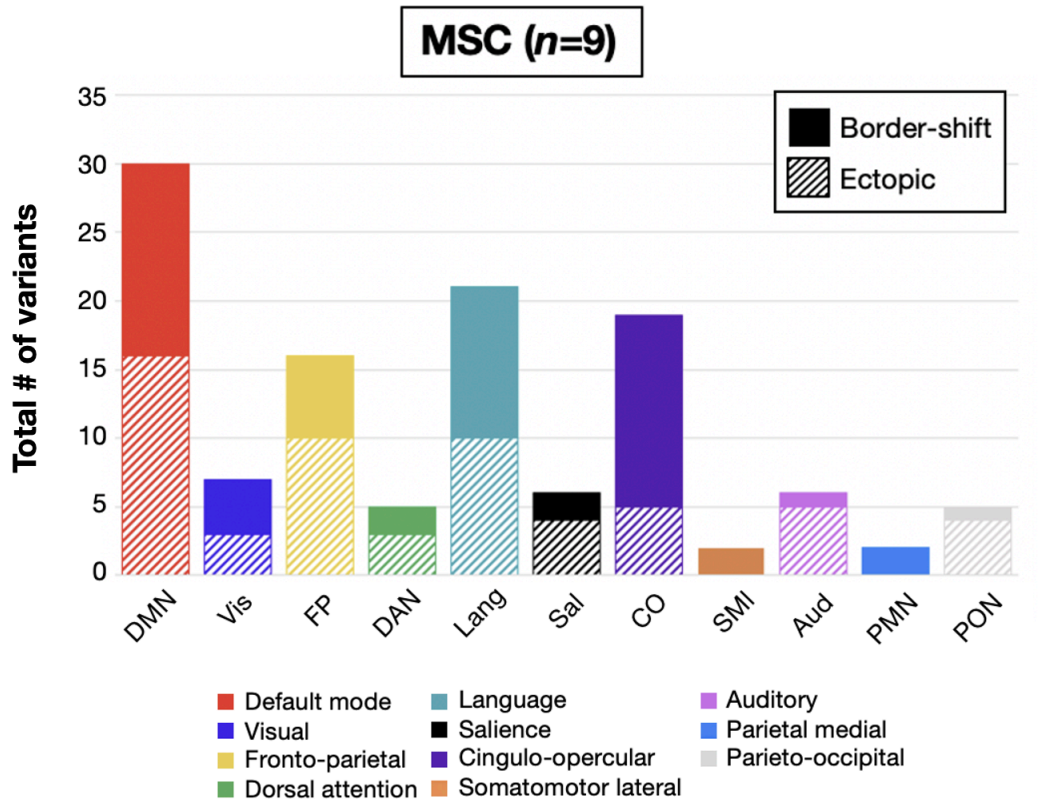

Supp. Fig. 6: Network distributions of border and ectopic variants in the MSC dataset. Each bar shows the number of variants associated with 12 common association networks in the MSC dataset, separated by whether variants were border shift or ectopic (similar to Fig. 3 in the main text).

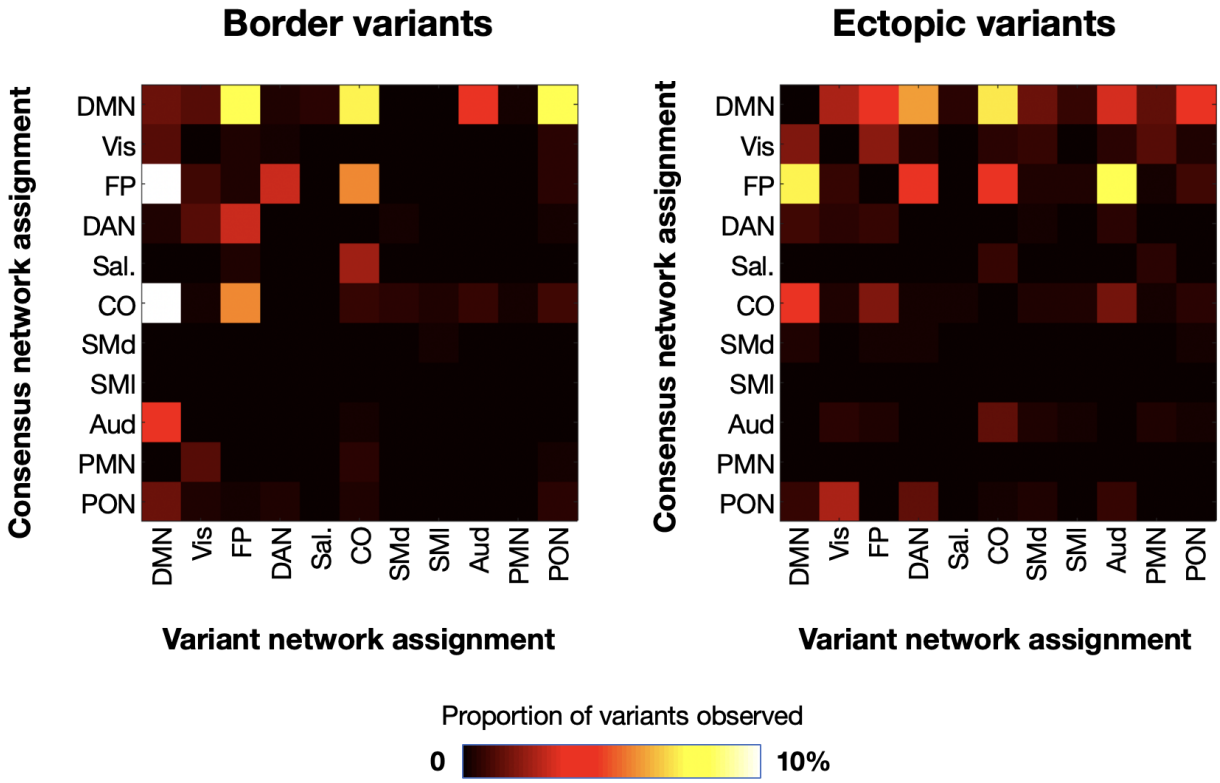

Supp. Fig. 7: Comparison of variant network assignment to consensus assignments at that location. For each border (left) and ectopic (right) variant, the figure displays the typical consensus network associated with a given variant's location (rows; defined as the modal network across variant vertices) versus the idiosyncratic network to which the variants were assigned in HCP participants. Values represent the raw percentage of variant "swaps" observed (i.e., out of all possible border or ectopic variants).

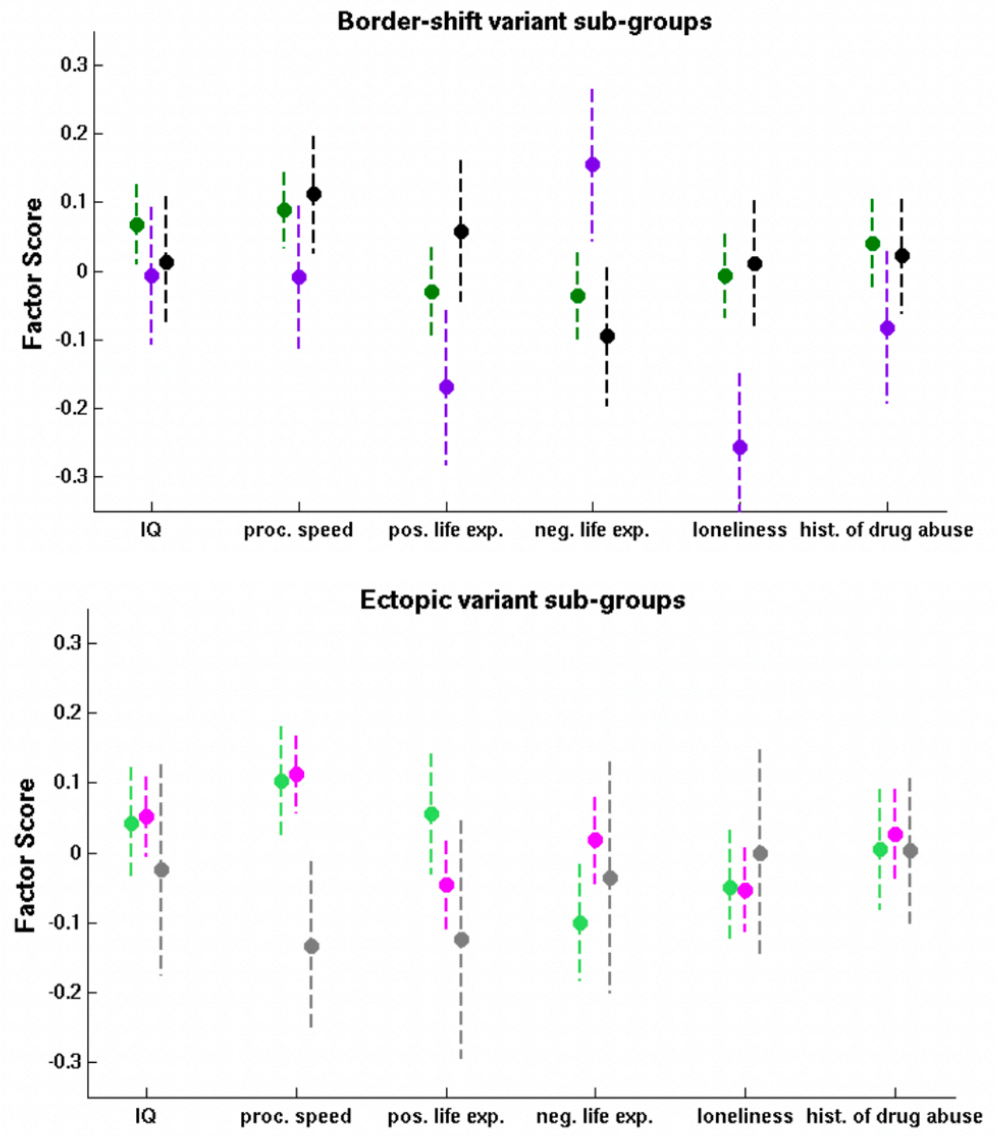

Supp. Fig. 8*: Behavioral differences between border-shift and ectopic variant sub-groups.* Results from previous work with network variants revealed small differences across two neuropsychological measures between sub-groups of individuals with similar variant connectivity profiles. An analysis similar to that conducted by Seitzman et al. (2019) was performed in order to explore a potential link between variants and behavior. Here, we assessed the relationship between variant sub-group membership and various HCP behavioral measures (collected outside of the scanner) with the goal of determining whether similar relationships exist for ectopic and border-shift variants. To do so, we used the exploratory factor analysis (EFA) of HCP behavioral factors from Seitzman et al (2019). This analysis reduced the number of behavioral variables of interest to six (IQ, processing speed, positive life experience, negative life experience, loneliness, and history of drug abuse). A one-way ANOVA was performed for each behavioral measure to assess differences between the sub-groups identified with only

ectopic intrusions or border shift variants respectively. When all six behavioral measures were compared between each identified sub-group from border-shift and ectopic variants, no significant differences between sub-groups were observed after FDR correction.

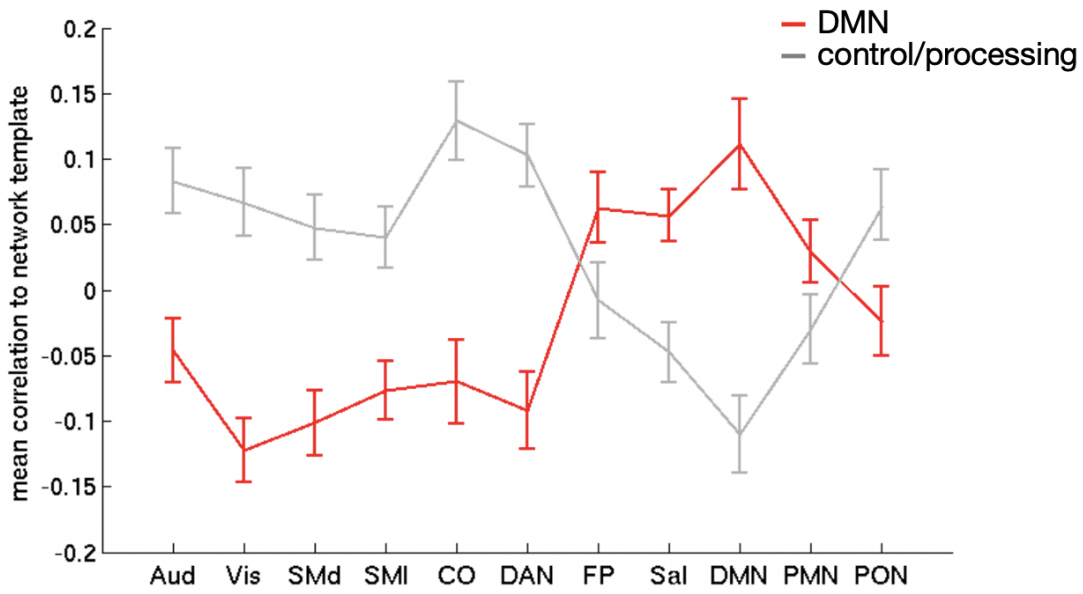

Supp. Fig. 9: DMN and control/processing sub-group profiles. In order to determine whether subjects consistently sorted into the same sub-group based on their border vs. ectopic variants, we matched participants into two reliable sub-groups that were identified across variant types in previous work (Seitzman et al., 2019): (1) a sub-group of individuals whose variants had high affinity to the DMN and (2) a sub-group of individuals with variants showing higher affinity to top-down control and sensorimotor processing systems. The network profiles for the two subgroups are shown above. These profiles were used as a template to group subjects by both their border and ectopic variants (see *Methods*).

REFERENCES

Gordon, E.M., Laumann, T.O., Adeyemo, B., Huckins, J.F., Kelley, W.M., and Petersen, S.E. (2016). Generation and Evaluation of a Cortical Area Parcellation from Resting-State Correlations. Cereb Cortex *26*, 288-303. 10.1093/cercor/bhu239.

Seitzman, B.A., Gratton, C., Laumann, T.O., Gordon, E.M., Adeyemo, B., Dworetsky, A., Kraus, B.T., Gilmore, A.W., Berg, J.J., Ortega, M., et al. (2019). Trait-like variants in human functional brain networks. Proc Natl Acad Sci U S A *116*, 22851-22861. 10.1073/pnas.1902932116.